



HAL
open science

Facies distribution and depositional cycles in lacustrine and palustrine carbonates: The Lutetian–Aquitanian record in the Paris Basin

Kévin Moreau, Simon Andrieu, Justine Briaïs, Benjamin Brigaud, Magali Ader

► To cite this version:

Kévin Moreau, Simon Andrieu, Justine Briaïs, Benjamin Brigaud, Magali Ader. Facies distribution and depositional cycles in lacustrine and palustrine carbonates: The Lutetian–Aquitanian record in the Paris Basin. *Depositional Record*, 2024, 10 (1), pp.124-158. 10.1002/dep2.264 . hal-04372428

HAL Id: hal-04372428

<https://hal.science/hal-04372428>

Submitted on 4 Jan 2024

HAL is a multi-disciplinary open access archive for the deposit and dissemination of scientific research documents, whether they are published or not. The documents may come from teaching and research institutions in France or abroad, or from public or private research centers.

L'archive ouverte pluridisciplinaire **HAL**, est destinée au dépôt et à la diffusion de documents scientifiques de niveau recherche, publiés ou non, émanant des établissements d'enseignement et de recherche français ou étrangers, des laboratoires publics ou privés.



Distributed under a Creative Commons Attribution 4.0 International License

Facies distribution and depositional cycles in lacustrine and palustrine carbonates: The Lutetian–Aquitainian record in the Paris Basin

Kévin Moreau¹  | Simon Andrieu^{2,3,4} | Justine Briais² | Benjamin Brigaud^{1,5} | Magali Ader⁶

¹Université Paris-Saclay, CNRS, GEOPS, Orsay Cedex, France

²BRGM, Orléans, France

³Department of Geoscience, Aarhus University, Aarhus C, Denmark

⁴Laboratoire de Géologie de Lyon: Terre, Planètes et Environnement, CNRS, Ecole Normale Supérieure de Lyon, Université de Lyon 1, Villeurbanne, France

⁵Institut universitaire de France (IUF), Paris, France

⁶Institut de physique du globe de Paris, CNRS, Université Paris Cité, Paris, France

Correspondence

Kévin Moreau, CNRS, GEOPS, Université Paris-Saclay, Orsay Cedex, France.

Email: kevin.moreau.arnage@gmail.com

Funding information

Bureau de Recherches Géologiques et Minières, Grant/Award Number: 2019-157; French Ministry of Research and Higher Education, Grant/Award Number: 2019-105

Abstract

The difficulty of correlating continental deposits hinders predicting lacustrine and palustrine carbonate facies variations in time and space. This study aims to understand better the factors governing these facies heterogeneities by measuring carbonate isotopes and conducting facies, petrographic and sequence stratigraphic analyses of the Lutetian–Aquitainian deposits of the Paris Basin, that record the transition from marine to lacustrine environments. Large-scale correlations enabled the definition of two lacustrine–palustrine carbonate facies models. (1) The coastal lacustrine system (Bartonian to Rupelian), consists of fine-grained brackish carbonate exhibiting episodic marine inputs during short-term relative sea-level maxima and evaporite sedimentation during relative sea-level minima. Lacustrine sediments differ notably from marine ones with more negative $\delta^{13}\text{C}$ and $\delta^{18}\text{O}$ compositions that co-vary and a biota adapted to low salinity conditions. In the associated palustrine environment, depositional sequences evolve upwards from micritic lacustrine deposits to nodular and then laminar calcretes. Microbial-coated grains and rhizoliths indicate biological processes during repeated subaerial exposure phases in sub-tropical to arid climates. (2) The inland lacustrine system (Rupelian and Aquitainian) was disconnected from the marine domain and showed evidence of microbial activity with microbial crusts and oncoidal rudstones. Facies rich in micritic intraclasts composed of palustrine and lacustrine facies indicate the reworking of already lithified sediments along the margins. In the palustrine domain, the calcrete facies are less abundant than breccias formed *in-situ* by desiccation, limestones with root traces, or organic-rich wackestones and marls. This system reflects a more temperate climate with more developed microbial structures and less exposed carbonates than the coastal lacustrine system. The southward migration of the depocentre and the transition from marine environments to (1) coastal and then (2) inland systems are controlled by uplift phases induced by Pyrenean and Alpine orogenesis.

This is an open access article under the terms of the [Creative Commons Attribution](https://creativecommons.org/licenses/by/4.0/) License, which permits use, distribution and reproduction in any medium, provided the original work is properly cited.

© 2023 The Authors. *The Depositional Record* published by John Wiley & Sons Ltd on behalf of International Association of Sedimentologists.

Third-order relative sea-level variations appear to control only short-term cycles in coastal systems.

KEYWORDS

Cenozoic, facies model, lacustrine, non-marine carbonate, palustrine, Paris Basin, stratigraphy

1 | INTRODUCTION

In continental systems, facies vary significantly, both spatially and temporally, making it difficult to predict and model them. This heterogeneity is partly explained by the fact that continental environments are more sensitive than marine environments to changes in accommodation space (Allen & Collinson, 1986; Bohacs et al., 2000). Variation in accommodation space is directly controlled by (1) vertical tectonic movements induced by subsidence and uplifts and (2) climate, which alters lake levels and sedimentation rates by varying inflow/evaporation ratios (Allen & Collinson, 1986; Bohacs et al., 2000; Alonso-Zarza, 2003). The respective influences of climate and tectonics on accommodation space and sedimentary facies variations are still difficult to disentangle, not least because of the incomparably more significant carbonate facies heterogeneity than that found on marine platforms (Della Porta, 2015; De Boever et al., 2017; Capezzuoli et al., 2022). Despite their significant variability, it is difficult to discriminate among deposits from nearby environments, such as palustrine and pedogenic facies due to similar sedimentary features (roots, desiccation cracks, etc.; Freydet & Plaziat, 1982; Wright & Tucker, 1991; Tandon & Andrews, 2001; Alonso-Zarza, 2003; MacNeil & Jones, 2006; Brasier, 2011).

Non-marine carbonates represent, by definition, “carbonate sediments that form and may be syn-depositionally transformed (“diagenetically altered”) under the strong influence of meteoric waters, including situations with various degrees of mixing with seawater, evaporative or basinal fluids” (De Boever et al., 2017). This definition, although generic, has limitations in ancient coastal environments since it lacks criteria for determining in which environments carbonates were deposited: non-marine (lacustrine, palustrine) or marine (lagoons). The coasts of the Yucatán, Florida and Bahamas platforms are a perfect example of the close spatial relationship that can exist between non-marine (mainly palustrine, brackish to freshwater environments) and marine (lagoon, beach barriers, reefs ...) carbonates (Platt & Wright, 2023). Moreover, foraminifera have even been found in Cenozoic and Quaternary lake deposits, attesting a marine water influence (Dye & Barros, 2005; Strotz, 2015; Lettéron et al., 2017; Pint et al., 2017; Fritz et al., 2018), while Warren and

Kendall (1985) suggest that the sulphate supply leading to gypsum precipitation in coastal salinas/playas comes from marine groundwater. The impact of the marine domain on coastal lacustrine and palustrine sedimentation can therefore play a significant role in sedimentation processes and requires further investigation.

Another question related to the impact of the marine domain on continental environments concerns the ability or otherwise to correlate marine and non-marine sedimentary series. Indeed, the sedimentation processes on continental systems are largely controlled by autocyclical parameters (river inflow and discharge, local climate, aquifer-level evolution, glacial storage, tides for very large lakes...) all depending on the evolution of continental systems controlled by allocyclical parameters (tectonics and climate; Allen & Collinson, 1986). Eustatic variations should not affect lakes or marshes. Nonetheless, MacNeil and Jones (2006) show that palustrine carbonates developed during sea-level fall in ancient coastal areas. In the same way, Platt and Wright (2023) suggest that palustrine deposits occurring in inland basins may have been influenced by sea level due to ephemeral connections with the marine domain. The coastal realm, even if predominantly non-marine, could therefore exhibit cyclicity similar to that of the marine realm.

Furthermore, there is difficulty in dating non-marine deposits due to (1) the poor preservation of fossils, (2) the scarcity of good stratigraphic fossils, and (3) the abundance of sedimentary hiatuses. This creates difficulty in establishing correlations in non-marine carbonates that prevent the precise characterisation of sedimentary architectures, further reinforcing the difficulty in understanding and predicting their facies continuity in the continental domain. Numerous studies have focussed on spatially constraining non-marine facies in extensional contexts, such as in lacustrine rift basins, where the difference in subsidence rates leads to profiles with steep slopes (Platt & Wright, 1991; Thompson et al., 2015). In these contexts, shallow high-energy platforms can develop on topographic highs, displaying shell or oncoïd accumulations, ooid shoals, mudflats, or wave-dominated sedimentary features (Platt & Wright, 1991; Mercedes-Martín et al., 2014; Thompson et al., 2015; Deschamps et al., 2020; Lettéron et al., 2022). There is less literature on basins in more stable tectonic contexts, such as intracratonic basins. In

these cases, depositional profiles are flatter and smoother, and the lake margins are more subject to variation in the lake water level that strongly depends on climate (Platt & Wright, 1991; Bohacs et al., 2000; Alonso-Zarza, 2003).

While depositional models have already been proposed for lacustrine systems, mostly on extensive contexts (Mercedes-Martín et al., 2014; Thompson et al., 2015; Deschamps et al., 2020; Lettéron et al., 2022), several questions remain. How do climate and tectonics influence lacustrine and palustrine carbonate facies in intracratonic basins? How does the relative position of the basin in relation to the coastline influence non-marine carbonate sedimentation and facies? What are the criteria for identifying lacustrine carbonates from lagoon carbonates? Do eustatic variations affect coastal lake systems? If so, do they allow us to correlate stratigraphic surfaces from the marine to the continental domain?

The Cenozoic carbonate deposits of the Paris Basin formed in marine and non-marine settings from the Lutetian to the Aquitanian (Eocene, Oligocene, Miocene). Their biostratigraphic fauna and flora have been closely studied, providing an excellent stratigraphic framework for answering some of the questions raised above (Abrard, 1925; Blondeau et al., 1965; Cavelier, 1969; Turland, 1974; Pomerol & Riveline, 1975; Gitton et al., 1986). However, most previous facies and stratigraphic works on the Cenozoic sedimentary rocks of the Paris Basin have focussed on the coastal and marine domains (Gély & Lorenz, 1991; Briais, 2015; Briais et al., 2016). Only a few (albeit detailed) studies have concentrated on interpreting non-marine carbonate facies (Ménillet, 1974; Guillemain, 1976; Freydet & Plaziat, 1982), where no magnetostratigraphy or chemostratigraphy is available. This study has the objective to determine facies and the depositional environments of both marine and non-marine Lutetian-Aquitainian carbonates of the Paris Basin. The relative controls of climate, tectonics and proximity of the coastline to the variety and distribution of non-marine carbonate facies are then discussed. For this purpose, a field and petrographic study was conducted to define facies and depositional environments. Based on pre-existing biostratigraphic data and by extending the pre-existing sequence stratigraphic framework to new outcrops and boreholes (Delhaye-Prat et al., 2005; Briais, 2015), large-scale cross-sections are proposed to reconstruct the geometries from the marine to lacustrine or palustrine domains. To constrain the hydrology and the type of water (marine vs. meteoric) where carbonate facies formed, oxygen and carbon stable isotopic data on carbonates were acquired. The main contribution of this study is to propose two facies models for lacustrine–palustrine environments corresponding to the newly defined coastal lake and inland lake systems. For each of these models, the study assesses the evolution of facies from the lake

depoecentre to the palustrine setting. Moreover, evidence is produced that both climate and geographic location control facies type and heterogeneity.

2 | GEOLOGICAL SETTING

The Paris Basin is an intracratonic sedimentary basin filled by Triassic to Quaternary deposits above a Cadomian to Variscan basement (Guillocheau et al., 2000). During the Cenozoic, a low subsidence phase occurred along E–W axes of subsidence until the late Eocene while NE–SW subsidence continued until the Miocene (Guillocheau et al., 2000; Briais, 2015). A number of compressive structures such as NW–SE-orientated folds and faults were active during these periods related to the Pyrenean collision, while NE–SW flexure is interpreted as a response to the Alpine collision (Robin et al., 1998; Guillocheau et al., 2000; Bourgeois et al., 2007; Briais, 2015).

From the Lutetian to the Aquitanian, the Paris Basin was dominated by carbonate and clastic sedimentation fluctuating from shallow marine to lacustrine and palustrine environments (Ménillet, 1974; Mégnien, 1980; Ziegler, 1990; Meulenkamp et al., 2000; Copestake et al., 2003; Londeix et al., 2014). Coastal environments, including estuaries, restricted marine domains, intertidal zones, supratidal zones, or lakes, were important depositional environments during this interval (Blondeau et al., 1965; Delhaye-Prat et al., 2005; Figure 1). This variety of depositional environments depends on the connection of the northern part of the basin with the marine domain via a NW–SE oriented channel (Figure 1A,B). This channel is recorded by littoral shelly sands between the Bray and Vigny anticlines (Morellet & Morellet, 1948; Pomerol et al., 1965; Mathelin & Bignot, 1989; Gély & Lorenz, 1991). The connection became less and less active from the Lutetian (Figure 1A,B) and was severed by the late Rupelian with the transition from estuarine and marine environments to lacustrine systems from the Bartonian (Figure 1C; Mégnien, 1980). The sedimentary material consists of carbonates, sands, marls, clays and gypsum evaporites deposited in shallow marine to lacustrine environments. Today, these deposits outcrop in the vicinity of Paris (Figure 1D). Brackish foraminifera, charophytes and palynomorphs were attributed to calcareous nannofossil assemblages (Calcareous Nannofossil Palaeogene NP and Neogene NN zones) in an effort to correlate non-marine and marine deposits by comparing palaeontological records with the neighbouring basins of Hampshire in the United Kingdom and Belgium (Blondeau et al., 1965; Le Calvez, 1970; Pomerol & Riveline, 1975; Aubry, 1985; Riveline et al., 1996). Five major episodes

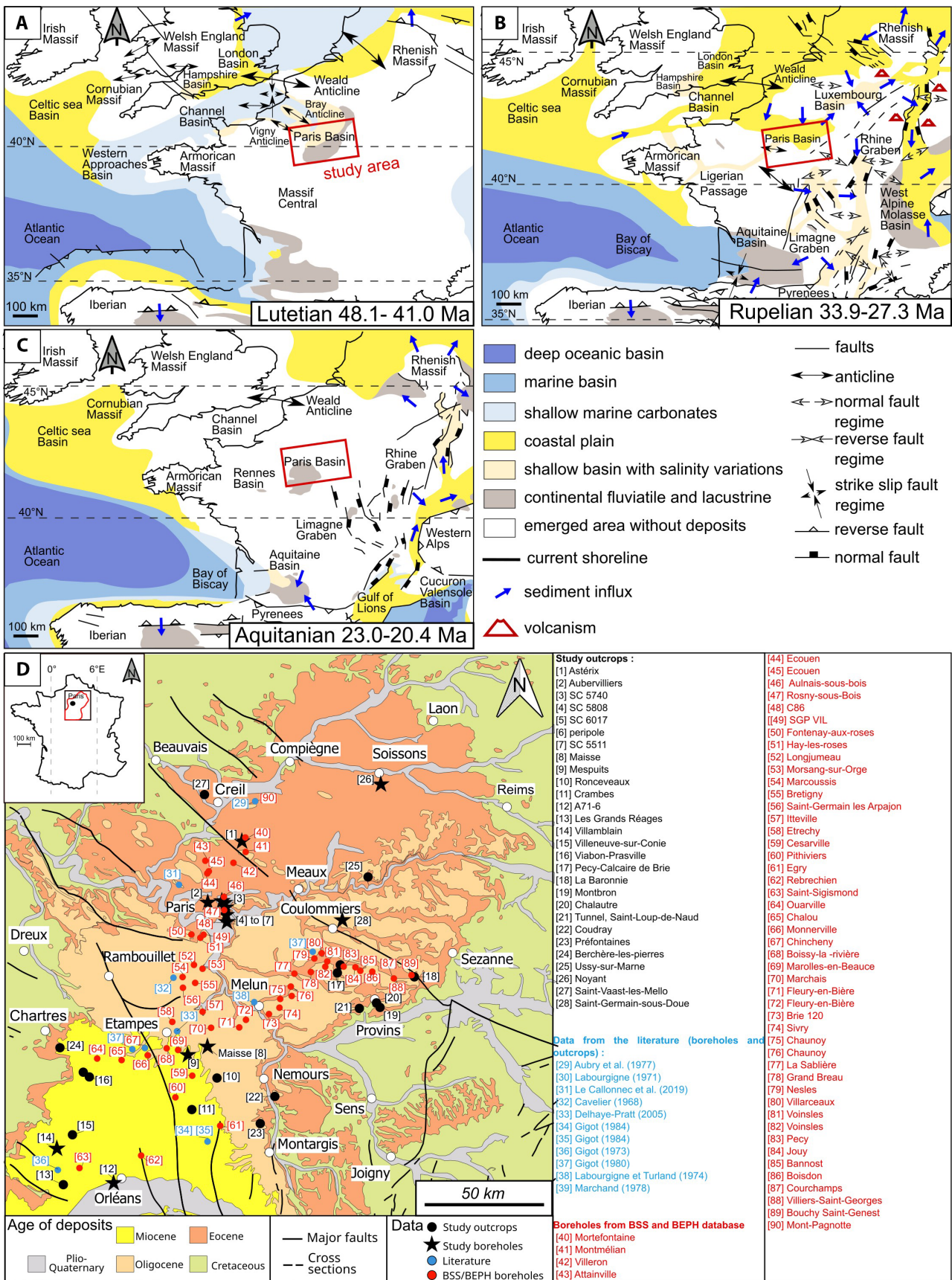


FIGURE 1 (A–C) Location of the study area on a palaeogeographical map of Western Europe during (A) the Lutetian, (B) the Rupelian, (C) the Aquitanian (Londeix et al., 2014; Copestake et al., 2003; Meulenkamp et al., 2000). The study area is highlighted by the red rectangle. (D) Location of the study outcrops and boreholes, outcrop and borehole data from the literature and databases, cross-sections in this study, and major faults intersecting the Cenozoic deposits in the Paris Basin.

of carbonate production are identified for the Lutetian–Aquitanian period, with N–S migration of the depositional environment (Figure 2): first, from the Lutetian to early Bartonian, marine bioclastic grainstones (Calcaire grossier Formation; equivalent to NP14b to NP15b zones) gave way to muddy marine facies (top of the Calcaire grossier and Marnes et Caillasses formations; equivalent to NP14b–NP16 zones; Figure 2) in the northern part of the basin (Abrard, 1925; Blondeau et al., 1965; Pomerol & Riveline, 1975; Toulemon, 1982). In the southern and eastern parts, planorbid limestones formed in freshwater environments (*Planorbis pseudoammonius*; Blondeau et al., 1965; Calcaire de Morancez, Calcaire de Darvault and Calcaire de Provins formations). Second, during the late Bartonian (equivalent to NP17 zone), deposition of a charophyte-rich lagoon–lacustrine limestone dominated (*Chara friteli*, *Gyrogona tuberosa* and *Raskyella vadaszi* zones; Calcaire de Saint-Ouen Formation) between short marine sandy episodes (Sables de

Mortefontaine and Sables de Cresnes-Monceau members). Third and fourth during the Priabonian to early Rupelian (equivalent to NP18, 19, 20, and 21 zones), lacustrine limestones poor in fossils were deposited in the southern and eastern parts of the basin (Calcaire de Champigny and Calcaire de Brie formations; Figure 2). Gypsum evaporites or marls accumulated in the central part of the Paris Basin during the Priabonian (Marnes et Masses de gypses Formation and Marnes blanches de Pantin Member; Mégnien, 1974; Turland, 1974), giving way to limestones or marls with marine species during the early Rupelian (Caillasses d’Orgemont Formation). Fifth, during the late Rupelian and Aquitanian, lacustrine carbonates were deposited in the southern part of the basin, between Chartres, Etampes and Montargis (Figure 1) with the Calcaire d’Etampes (late Rupelian, *Chara microcera*, equivalent to NP24 zone, Riveline, 1983) and the Calcaire de Beauce formations (Aquitanian, *Stephanochara bertotensis* zone; Figure 2)

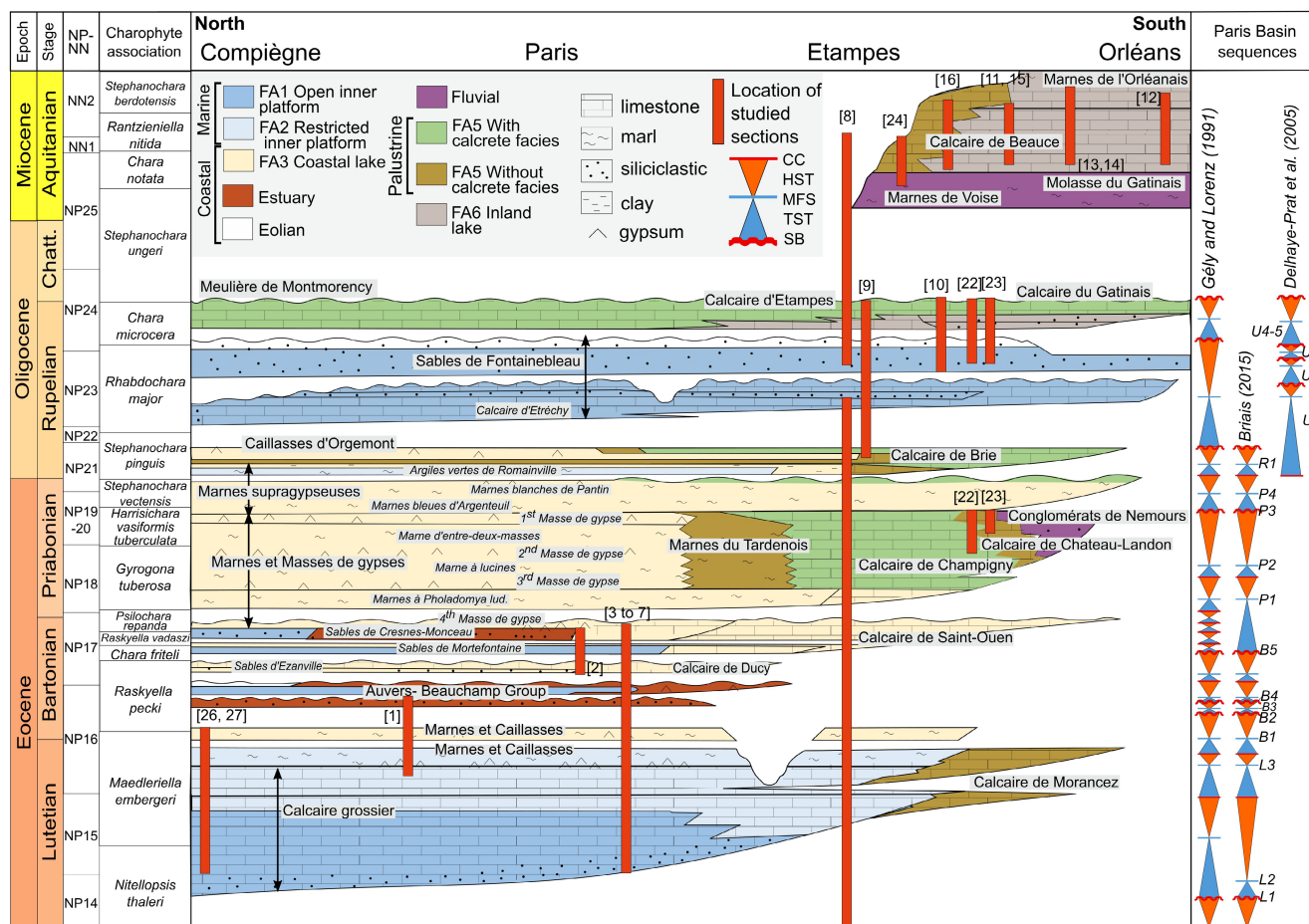


FIGURE 2 Schematic lithostratigraphic illustration following a NE–SW cross-section across the study area (modified after Gély, 2016). Members are written in italics. Palaeoenvironmental interpretations are from Mégnien (1980), Briais (2015), and this study. The names of the localities are given in Figure 1D. NP–NN: Calcareous Nannofossil zones for the Palaeogene (NP) and Neogene (NN) epochs. The following abbreviations are used for short-term sequence stratigraphic surfaces and systems tracts: CC: Correlative conformity; HST: Highstand Systems Tract; MFS: Maximum Flooding Surface; TST: Transgressive Systems Tract; SU: Subaerial Unconformity; U: Unit.

due to the separation of the basin from the marine domain to the north (Denizot, 1927; Cavelier, 1969; M nillet, 1974; Guillemain, 1976; Lozouet, 2012). A sedimentary hiatus is recognised during the Chattian, between these two units (Pomerol, 1989).

These five major episodes of carbonate production are separated by four siliciclastic episodes (Figure 2): coastal sands of the Auvers-Beauchamp group (early Bartonian; M gnien, 1980; Briais, 2015) and the Sables de Cresnes-Monceau Member (late Bartonian); marl deposits with brackish to marine fauna of the Marnes   *Pholadomya ludensis* Member (early Priabonian; Pomerol et al., 1965); the Marnes bleues d'Argenteuil Member (late Priabonian) and the Argiles vertes de Romainville (early Rupelian) Member; and finally a sandy siliciclastic marine episode topped by aeolian dunes with the Sables de Fontainebleau Formation (Rupelian; Alimen, 1936; Gitton et al., 1986; Delhaye-Prat et al., 2005).

Four long-term cycles and 22 short-term depositional cycles were established by previous work in the Lutetian–Aquitainian interval of the Paris Basin (Delhaye-Prat et al., 2005; Briais, 2015). The major stratigraphic surfaces that can be recognised throughout the basin and define these cycles are detailed in the supplementary material.

3 | METHODS AND MATERIAL STUDIED

3.1 | Core description, facies and petrography

This study is based on the detailed examination of 17 outcrops in the eastern and southern part of the basin and 18 boreholes located in Paris [locations 3–9, 12, 25 and 28 in Figure 1D]. The data set is completed with gamma-ray well-logs (<http://infoterre.brgm.fr/> and <http://www.minergies.fr/fr>) from 51 boreholes available online from the French Geological Survey databases, supplemented by 11 outcrop or borehole sedimentary logs from 1:50000 scale geological maps (Marchand, 1968; Labourguigne, 1971; Labourguigne & Turland, 1974; Gigot, 1973, 1980, 1984) and other studies (Cavelier, 1968; Aubry et al., 1977; Delhaye-Prat et al., 2005; Le Callonnec et al., 2018). Outcrops and boreholes have been described in detail using the classifications of Dunham (1962) and Embry and Klovian (1971) for texture, and the commonly used terminology for non-marine facies based on the structure of specific facies such as calcretes or microbial carbonates (Platt, 1989; Platt & Wright, 1991; Alonso-Zarza & Wright, 2010a; Gierlowski-Kordesch, 2010; Alonso-Zarza

et al., 2011; Roche, 2020). Classification of microbial-rich build-ups after Vennin et al. (2021) is used for the description of microbial features in sedimentary facies. Facies and microfacies have been characterised based on their lithology, texture, sedimentary structures and component grains observed on macro samples and on 205 thin sections.

3.2 | Sequence stratigraphy and cross-sections

To understand the depositional geometries and to establish stratigraphic cross-sections, outcrops and boreholes were interpreted in terms of sequence stratigraphy. Three types of stratigraphic surfaces used in marine areas can be applied to continental deposits (Hanneman & Wideman, 2010): subaerial unconformities, correlative conformities and maximum flooding surfaces. Units are bounded by sequence boundaries (subaerial unconformities and their correlative conformities), which represent the shallowest environment recorded within a sequence and coincide with shifts in stacking patterns between shallowing-upward and deepening-upward trends (Strecker et al., 1999; Changsong et al., 2001; Keighley et al., 2003; Hanneman & Wideman, 2010; P rez-Rivar z et al., 2018; Deschamps et al., 2020; Guan et al., 2021; Melo et al., 2021; Lett ron et al., 2022). Subaerial unconformities were identified by surfaces characterised by features such as erosion karstification or palaeosoils occurrence—whereas correlative conformities are surfaces that were not (Hanneman & Wideman, 2010). Maximum flooding surfaces (MFS) represent the deepest deposits encountered within a sequence and mark the shift between deepening-upward and shallowing-upward trends (Hamilton & Tadros, 1994; Keighley et al., 2003). In the succession of palustrine deposits encountered in this study, the beds with the least evidence of pedogenic modifications were interpreted as MFS, recording the periods when the water level was highest. Subaerial unconformities, correlative conformities and maximum flooding surfaces separate transgressive systems tracts, characterised by deepening-upward facies, and highstand systems tracts, characterised by shallowing-upwards facies (Strecker et al., 1999; Bohacs et al., 2000; Changsong et al., 2001; Keighley et al., 2003; Bohacs et al., 2007; Deschamps et al., 2020; Guan et al., 2021). The nomenclature of the short-term and long-term surfaces used in this work for the Cenozoic of the Paris Basin was initially defined by Briais (2015).

Two stratigraphic cross-sections were constructed using the outcrops and boreholes listed in Figure 1D. The two cross-sections intersect at the Maisse borehole [location 8] for which detailed sedimentary description

and gamma-ray well-log interpretation were undertaken. This allows sedimentary facies and stratigraphic sequences to be matched with gamma-ray logs. This matching is used as a reference for interpreting other gamma-ray logs in terms of sedimentary facies/facies associations and then to establish correlations between sedimentary logs and well logs. The first cross-section is oriented north–south from the Mont-Pagnotte borehole [location 29 in Figure 1D] to Orléans [12] by way of Paris. The second one is oriented east–west, extending from Baronnie quarry [18] to Villermain quarry [13]. The age model of the depositional sequences relies on (1) the biostratigraphic fauna (foraminifera, charophytes, palynomorphs, dinocysts, malacofauna and mammals) identified in previous studies in sections from Creil to Etampes (N–S cross-section, Cavalier, 1968; Pomerol & Riveline, 1975; Aubry et al., 1977) and (2) correlation of these sequences with the ones defined in the Briaux cross-sections (2015), which relate to biostratigraphically well-anchored zones in the north of the basin. For that, the east–west cross-section provided here intersects those of Briaux (2015) between locations 71 to 78 (Figure 1D).

3.3 | Stable isotope analyses ($\delta^{13}\text{C}$ and $\delta^{18}\text{O}$)

The Cenozoic carbonates of the Paris Basin were only slightly buried (a hundred metres at most) implying limited burial diagenesis of the micrite. Carbon and oxygen isotope analyses were conducted on 43 micritic carbonate samples collected in the Maise well [location 8 on Figure 1D] in deposits dated from the Lutetian (top of the Calcaire grossier Formation) to the end of the Rupelian (Calcaire d'Etampes Formation; Supplementary data). The micrites all have a low-magnesium calcite mineralogy (>1% MgO). They are autochthonous micrites except for the palustrine facies where pseudomicrites are present (Flügel & Munnecke, 2010). Carbonates (2.5 mg) were sampled by micro-drilling on newly sawn faces in homogeneous micritic areas, with the powder placed in sealed tubes and dissolved using H_3PO_4 to produce CO_2 . Carbon and oxygen isotopic compositions of the evolved CO_2 were measured using a gas chromatograph coupled to a GVInstruments Analytical Precision 2003 mass spectrometer at the Université Paris Cité (Institut de Physique du Globe de Paris, Paris, France) (for method details see Assayag et al., 2006). Three internal standards (Rennes 1; Merck and Accros) were used to convert raw isotope values into $\delta^{18}\text{O}_{\text{PDB}}$ and $\delta^{13}\text{C}_{\text{PDB}}$ values and evaluate the reproducibility of the analyses. The isotopic values represent the mean of four analyses made for each sample. The

external reproducibilities (1σ) for $\delta^{13}\text{C}$ and $\delta^{18}\text{O}$ values are 0.1% and 0.2% respectively.

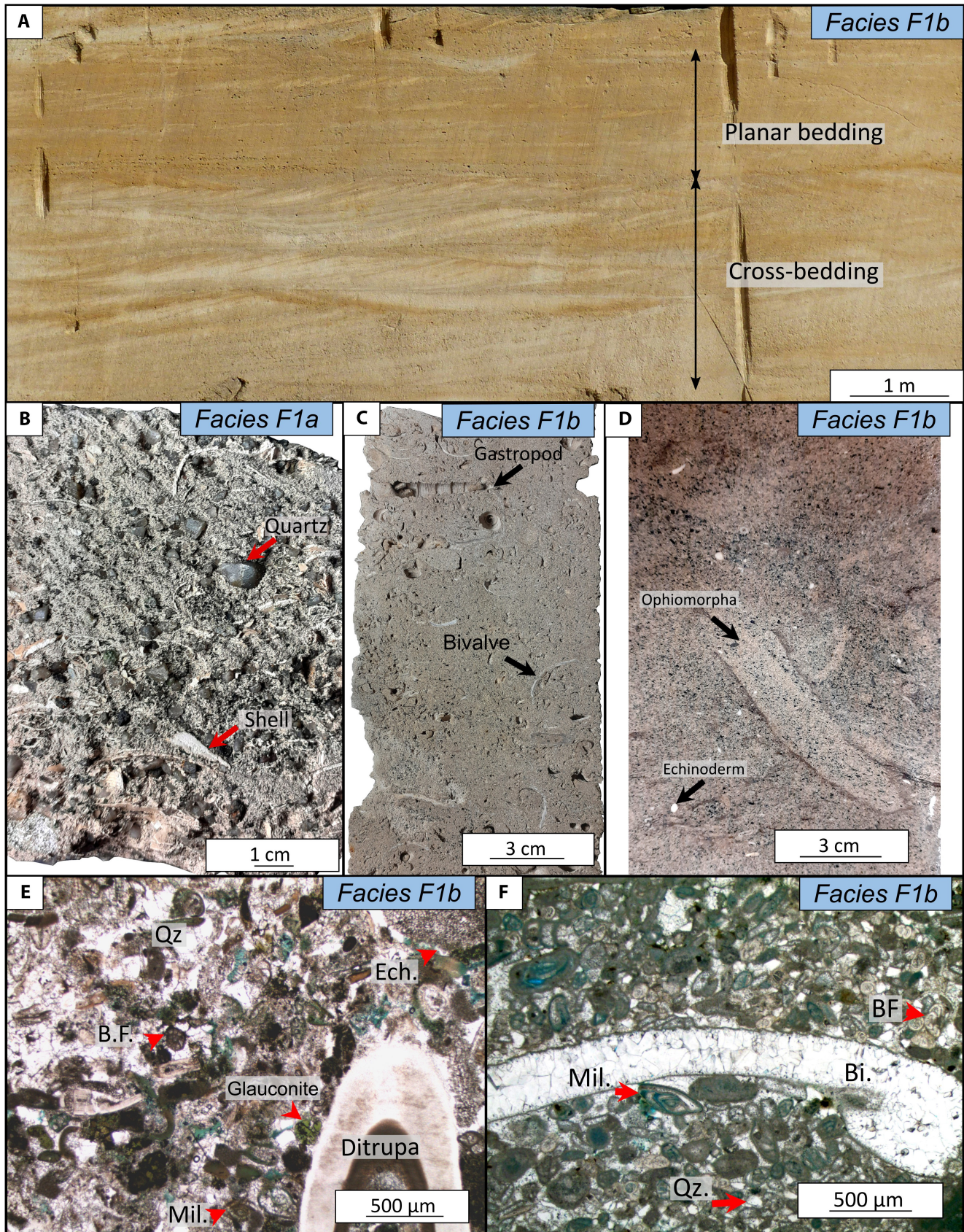
4 | RESULTS: DEPOSITIONAL ENVIRONMENTS AND SEDIMENTARY FACIES

Thirty-two sedimentary facies were grouped into six depositional environments: (1) the open marine inner platform for facies deposited in a high hydraulic energy marine setting above the fair-weather wave base; (2) the restricted marine domain for facies deposited in calm and shallow marine environments with varying salinity; (3) the coastal lake for facies deposited under fresh to brackish waters in the coastal environment with rare sporadic connections with the marine domain; (4) the floodplain; (5) the palustrine environment, recording the deposition of carbonates under fresh or brackish water which were then subjected to subaerial exposure and modification of the sediment; and (6) the inland lake, never connected to a marine setting. Observations, descriptions and isotopic data are presented in detail below. A summary table is given in the supplementary material.

4.1 | Facies association FA1 Open-marine inner platform

This facies association contains granular bioclastic limestones with two distinctive facies: a siliciclastic and foraminifera rudstone (facies F1a) and a bioclastic grainstone or rudstone (facies F1b) (Figure 3A through F). The biota is composed of gastropods, bivalves, annelids (serpulids and ditrupes), echinoderms, and a wide variety of benthic foraminifera (nummulitids, orbitolinids, miliolids, etc.). Based on previous studies, bryozoans, sponges, brachiopods, fishes or turtles have also been found in these facies in the Paris Basin (Merle, 2008). Siliciclastic and foraminifera rudstones (facies F1a) present *Thalassinoides* burrows while bioclastic grainstones display *Ophiomorpha* bioturbations (facies F1b). Facies F1a, which is coarser than facies F1b, presents nummulites (often oriented), erosion gullies and erosive surfaces. Facies F1b shows cross bedding in dunes ranging from 10 cm to 1 m in height (types II to IV of Allen, 1980), planar bedding (Figure 3A) or wave ripples. The smallest dunes more frequently have reactivation surfaces.

The marine biota, the sedimentary structures, the common bioturbations (Figure 3D) and the large quantity of detrital quartz, all suggest a well-oxygenated open marine domain with a high energy wave-dominated or tide-dominated environment located above the fair-weather wave base



(Briaes, 2015). Dunes in facies F1b indicate an open marine environment between the subtidal and the intertidal domains while cross-bedding alternating with planar bedding

marks high energy tidal flat environments. Facies F1a indicates a shoreface environment further to the shoreline where storm events are recorded (Pemberton et al., 1992).

FIGURE 3 Open marine inner platform facies association FA1. The numbers indicated [#] correspond to the location of the boreholes and sedimentary sections in [Figure 1](#). (A) Quarry face revealing cross-bedding in dunes and planar bedding; Facies F1b; Calcaire grossier Formation, Lutetian [27]. (B) Sandy rudstone with coarse quartz and shell fragments; Facies F1a; Calcaire grossier Formation, Lutetian [5]. (C and D) Rudstone and grainstone with marine bivalves, gastropods, echinoderms and foraminifera, see the bioturbation (*Ophiomorpha*) in picture D; Facies F1b; Calcaire grossier Formation, Lutetian [3 and 6]. (E) Bioclastic grainstone in thin sections with quartz (Qz), benthic foraminifera (B.F.), miliolids (Mil.) and echinoderms (Ech.); Facies F1b; Calcaire grossier Formation, Lutetian [6]. (F) Same facies as picture D with bivalves (Bi.); base of the Sables de Fontainebleau Formation, Rupelian [8].

This facies association is abundant in the Calcaire grossier Formation (Lutetian) and at the base of the Sables de Fontainebleau Formation (Rupelian).

4.2 | Facies association FA2 Restricted marine inner platform

Petrography and sedimentary structures—Seven facies compose this association: (1) grainstone/packstone with miliolids (facies F2a) ([Figure 4A,B,C](#)), (2) alternations of foraminifera-rich wackestone and grainstones (facies F2b) ([Figure 4A,D](#)), (3) bioturbated floestone with a wackestone matrix (facies F2c) ([Figure 4E,F](#)), (4) alternations of dolomite and wackestone with foraminifera and storm wash-over (facies F2d) ([Figure 4G,H](#)), (5) alternations of miliolid grainstone and green marls (facies F2e) ([Figure 4I](#)), (6) alternations of gypsum and mudstone/wackestone levels (facies F2f) ([Figure 4J](#)), and (7) bioturbated mudstone (facies F2g) ([Figure 4K](#)). They correspond to centimetre-sized to decimetre-sized muddy limestone alternations with low faunal diversity (benthic foraminifera, dasyclads, echinoderms, gastropods, bivalves) and less detrital input than facies association FA1. Beds are planar or present metre-scale undulations ([Figure 4L](#)). Marine foraminifera families identified in these facies are, among others, Calcarinidae, Miliolidae, Fabulariidae, Polymorphinidae or Valvulinidae. Marine-brackish families are also present, such as Bolivinidae, Buliminidae, Discorbidae, Elphidiidae or Rosalinidae.

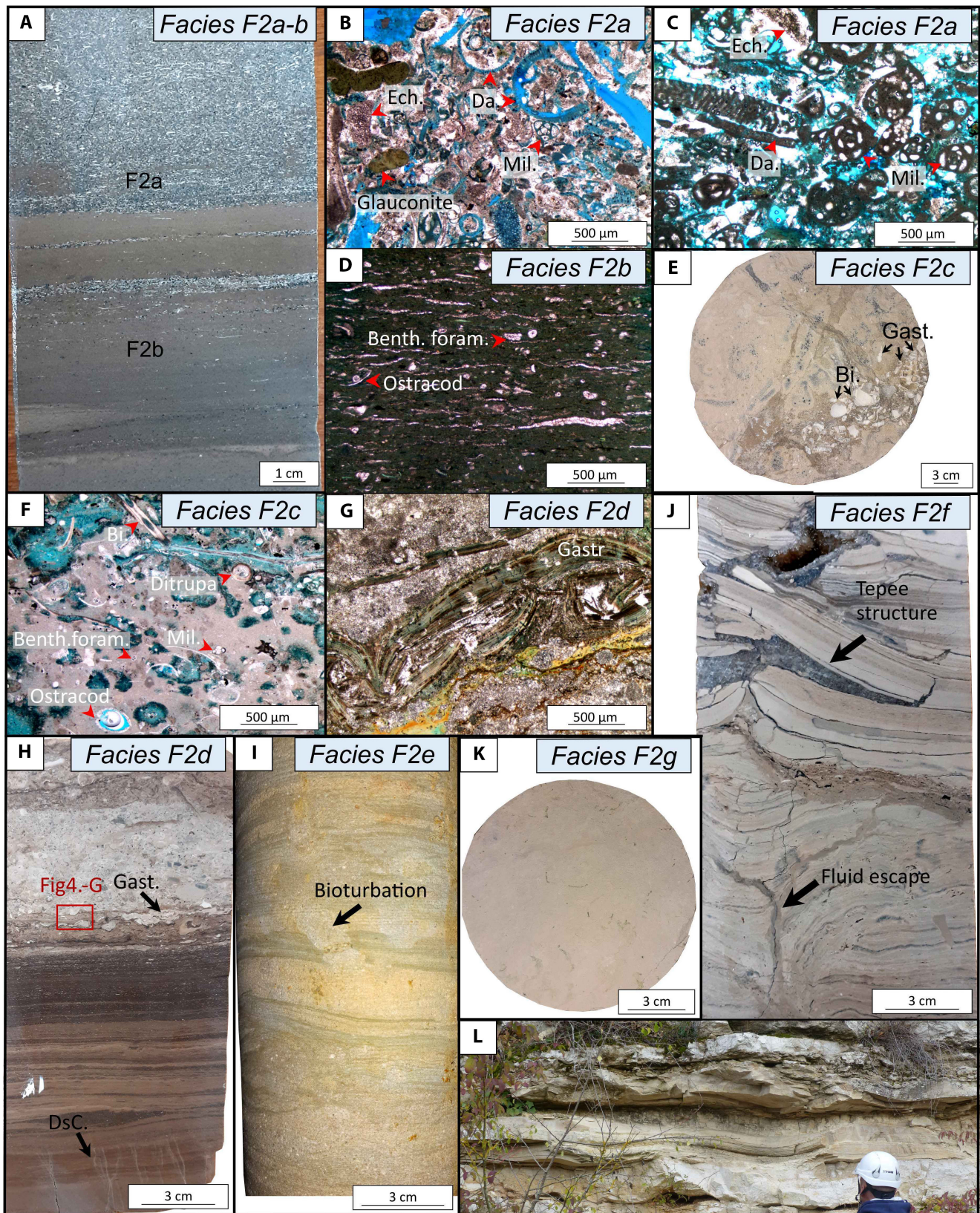
All these facies show few detrital grains, sometimes abundant bioturbations, laminations and alternation between muddy and granular lamina and/or beds, indicating fluctuating hydrodynamic energy from low to moderate energy environments, typical of restricted marine environments (Wilson, 1974; Arribas et al., 2004). The foraminifera assemblage characterises a marine environment with salinity fluctuations. The low biota diversity is dominated by miliolids and dasyclad algae, which suggests a protected marine environment such as an inner lagoon (Wilson, 1974; Langer & Lipps, 2003; Amao et al., 2016). Alternating muddy and shelly beds suggests deposition during storm wash-overs. In facies F2f, alternating gypsum and mudstone/wackestone with tepee structures indicates a supratidal environment along the margin, subjected to

alternating periods of flooding and then exposure during dry episodes (Kendall & Warren, 1987).

Oxygen and carbon isotopes—Isotopic values range from -4.6 to 1.1‰ for $\delta^{13}\text{C}$ and from -4.3 to 1.9‰ for the $\delta^{18}\text{O}$ (mean value of -2.2 and -1.2‰ , respectively), i.e., close to the range of non-recrystallised marine fossils obtained from marine molluscs from the Paris Basin (Huyghe, 2010) and from ostracods from the Hampshire Basin (Marchegiano & John, 2022), which, for a similar age, range from -2.5 to 1.5‰ for the $\delta^{13}\text{C}$ and from -5 to -0.5‰ for the $\delta^{18}\text{O}$ ([Figure 5](#)). This is consistent with the marine origin mentioned before. Some micrites (especially in facies F2e and g) exhibit variable oxygen isotopic compositions with some positive values, showing fluctuations in water chemistry during phases of evaporation. This association is exclusive to the upper part of the Calcaire grossier and the Marnes et Caillasses formations (Lutetian to early Bartonian).

4.3 | Facies association FA3 Coastal Lake

Petrography and sedimentary structures—This facies association consists of five facies showing rare sporadic connections of the basin with the marine domain: (1) alternating gypsum limestones and marls (facies F3a) ([Figure 6A,B,C](#)), (2) euryhaline foraminifera wackestone to mudstone (facies F3b) ([Figure 6D,E](#)), (3) shell rich packstone (facies F3c) ([Figure 6F](#)), (4) varves (facies F3d), and (5) gypsiferous marls (facies F3e). Facies F3a is locally composed of alternating gypsum, millimetre-scale planar microbial laminae, or calcite dendrites in a micritic matrix ([Figure 6A,B,C](#)). The gypsum crystallised as saccharoidal, lenticular or dendritic forms and is sometimes recrystallised in calcite or in silica. Facies F3b, F3c and F3d present a biota of ostracods, euryhaline foraminifera (families: Bolivinidae, Buliminidae, Discorbidae, Nonionidae, and Rosalinidae; genus: *Elphidiella* and *Caucasina*), gastropods, bivalves and charophytes ([Figure 6D,E,F](#)). The varve facies F3d corresponds to alternating limestone beds several tens of centimetres thick and thin clayey interbeds. The fossil assemblage in the gypsiferous marls F3e consists of brackish to marine species (Corbulidae, Turritellidae, Potamididae families) associated with charophytes in the northern part of the basin. However, they show an affinity



for brackish to freshwater environments (Lymnaeidae, Planorbidae, Truncatellidae families with genus *Nystia*) in the southern part.

These mud-rich facies with few detrital grains (>10%) indicate a restricted depositional environment with low

terrestrial input. The fossil assemblage is characteristic of a brackish to freshwater environment with fluctuating salinity (mostly mesohaline to oligohaline conditions) in coastal environments like estuaries, lagoons and coastal lakes (Plaziat, 1993; Dye & Barros, 2005; Strotz, 2015; Pint

FIGURE 4 Restricted marine facies association FA2. The numbers indicated [#] correspond to the location of the boreholes and sedimentary sections in Figure 1. (A) Horizontal alternations of bivalve-rich grainstone (facies F2a) and wackestone with foraminifera (facies F2b); Calcaire grossier Formation, Lutetian [6]. (B) Grainstone with miliolids; Facies F2a: miliolidae (mil.), dasycladial algae (da.), echinoderms (ech.), glauconite and quartz; Calcaire grossier Formation, Lutetian [6]. (C) Same facies as picture B; Calcaire grossier Formation, Lutetian [3]. (D) Wackestone with foraminifera; Facies F2b: benth. Foram: benthic foraminifera; Calcaire grossier Formation, Lutetian [6]. (E and F) Floatstone with large gastropods (gast.) and bivalves (bi.) in a wackestone matrix; Facies F2c with foraminifera, bivalves, ostracods and ditrupes, miliolids (Mil.) and benthic foraminifera (benth. Foram.). Bivalves are marine species (Veneridae); Calcaire grossier Formation, Lutetian [8]. (G and H) Alternating dolomite (dol.) and wackestone with foraminifera subjected to turbation by a tempestite with crushed gastropods (gast.). Note the desiccation cracks (DsC) at the bottom of the sample; Facies F2d; Marnes et Caillasses Formation, Lutetian–Bartonian [1]. (I) Alternating cross-bedded and bioturbated green marls and grainstone with foraminifera; Facies F2e; Calcaire grossier Formation, Lutetian [26]. (J) Alternating mudstone to wackestone layers with fluid escape and tepees; Facies F2f; sparite has precipitated between the laminae; Marnes et Caillasses Formation, Lutetian–Bartonian [1]. (K) Bioturbated mudstone; Facies F2g; green clay fragments are present; Calcaire grossier Formation, Lutetian [8]. (L) Alternating marls and mudstones with undulating bedding; Facies F2g; Marnes et Caillasses Formation, Lutetian–Bartonian [27].

et al., 2017; Fritz et al., 2018; Lettéron et al., 2018). These salinity variations are supported by the presence of gypsum levels in the depositional record.

Oxygen and carbon isotopes—Isotopic values range from -7.0 to $-2.3‰$ for the $\delta^{13}\text{C}$ and from -6.2 to $1.7‰$ for the $\delta^{18}\text{O}$ (means of -5.6 and $-3.5‰$, respectively; Figure 5). The isotopic composition of the micrite clearly distinguishes this environment from a restricted marine setting since its $\delta^{13}\text{C}$ and $\delta^{18}\text{O}$ values are more negative and within the range of open lakes (Talbot, 1990). This is best interpreted here as reflecting a higher contribution of meteoric waters (Allan & Matthews, 1982; Talbot, 1990).

Synthesis—Facies association 3 therefore presents mud-dominated carbonate with a low detrital content, a dominance of brackish species, and records meteoric isotope values. These observations are interpreted as indicating a coastal lake environment. The varve facies F3d represents the deeper and/or calmer part of the coastal lake whereas the shell packstone of facies F3c indicates moderate hydrodynamic energy with local accumulation of shells along the lake margin (Gierlowski-Kordesch, 2010). Facies F3a with gypsum levels and microbial mats indicates saline water deposits in a playa-like environment (Schreiber, 1988; Rouchy et al., 2001; Flügel & Munnecke, 2010). These gypseferous marls (F3e) are most influenced by marine incursions, as shown by the common occurrence of marine species. Some levels composed by this facies even show a marine environment like lagoons. This facies association made up the limestone and marl formations in the centre and the northern part of the basin during the Bartonian, Priabonian and early Rupelian.

4.4 | Facies F4 Floodplain

The floodplain is represented by only one facies in the Paris Basin: coarse to fine sandy clays. This facies is present at the base of the Lutetian deposits. It consists

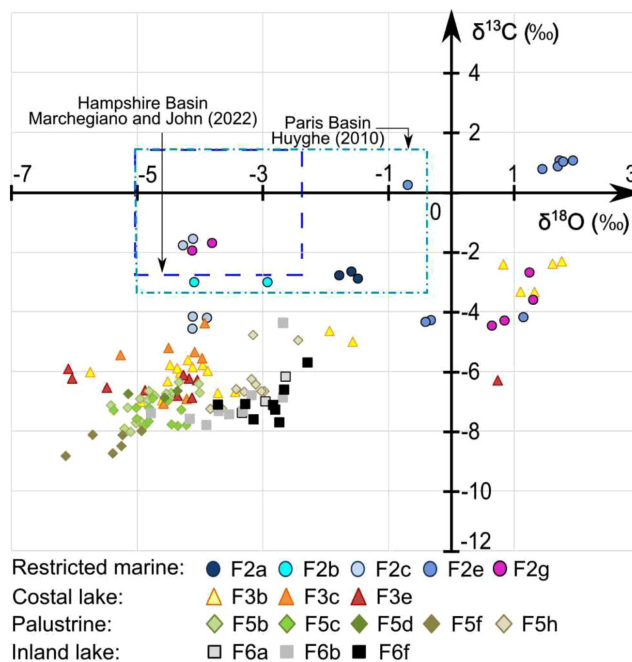


FIGURE 5 Cross-plot of stable carbonate isotopic composition ($\delta^{13}\text{C}$ and $\delta^{18}\text{O}$ values vs PDB) of micrite for marine, lacustrine and palustrine facies of the Cenozoic of the Paris Basin. Although some of the facies analysed show patches of sparitic cements or grains, the analyses were systematically carried out on micrite to reduce the impact of diagenesis on isotopic signals. The marine isotopic domain is given by the two blue rectangles based on the isotopic composition of ostracods from the Hampshire Basin (Marchegiano & John, 2022) and marine molluscs from the Paris Basin (Huyghe, 2010).

of bioturbated, brownish sandy clays to marls with terrestrial gastropods and sinuous vertical millimetre-wide bioturbations with a fine, organic-rich centre interpreted as ancient roots. This facies is present above erosional surfaces.

This facies is interpreted as floodplain associated with fluvial systems, marking the transgression of the Lutetian deposits above the Ypresian sedimentary formations.

4.5 | Facies association FA5 Palustrine environment

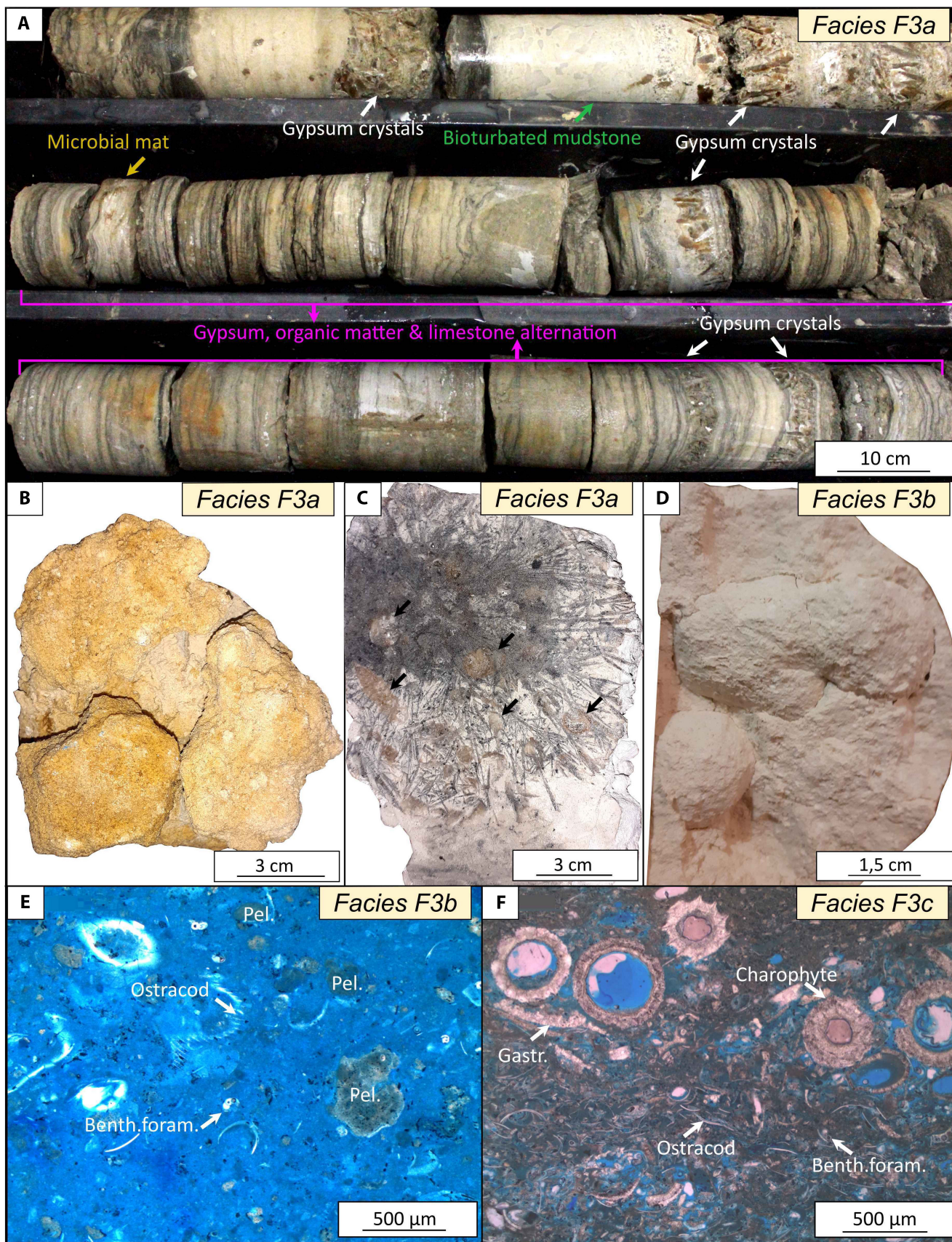
Petrography and sedimentary structures—The palustrine facies association is composed of eight facies displaying abundant subaerial exposure markers such as desiccation cracks or pedogenetic processes: (1) tubular limestones (facies F5a; Figure 7A,B), (2) nodular brecciated limestones (facies F5b, Figure 7C,D,E), (3) laminar brecciated limestones (facies F5c, Figure 7F), and chalky altered limestones (facies F5d, Figure 7G), (5) peloidal grainstones (facies F5e, Figure 7H,I), (6) *in-situ* brecciated limestones (facies F5f, Figure 7J,K,L), (7) organic-rich wackestone and marls with reworked intraclasts (facies F5g, Figure 7M), and (8) alternating mudstone and wackestone with root traces (facies F5h, Figure 7M,N). Facies F5a to F5d present intense subaerial exposure leading to extensive transformation of the primary sediment, which is difficult to recognise in some cases. Fauna is either absent or limited to rare ostracods. In facies F5b and F5c, intraclasts are mainly desiccated, displaying a jigsaw-puzzle structure. They are locally silicified by opal A, microcrystalline quartz or chalcedony. In thin section, facies F5a to F5c show alveolar-septal structures (Figure 7F), coated grains with micritic agglutinated fabrics or concentric microbial laminations (Figure 7C,D), rhizoliths and clotted micrite. Tubular voids interpreted as rootlet moulds and rarely preserved polygonal white or brownish prisms (*Microcodium*) extend throughout the matrix and the intraclasts (Figure 7B,C,F). Micrite laminae with desiccation cracks, fenestral fabrics and rootlet moulds making up the laminar brecciated limestones without any significant change in thickness (Figure 7F). A micritic matrix or a sparitic calcitic cement separate the clasts, while vadose calcitic cements develop in the porosity (Figure 7E). Facies F5e to F5h also present markers of subaerial exposure, although these are notably less important than in facies F5a–d. The top of the beds are often irregular but well recognisable in outcrops. The primary sediment is partly preserved and can be identified and described. Gastropods and ostracods are common, charophytes are locally present but rare, and former roots are abundant in the upper part of some

beds. Sometimes, the presence of laminated structures lying horizontally within the intraclasts confirms that the clasts have not been remobilised in *in-situ* brecciated limestones (facies F5f; Figure 7J). In Figure 7J, they also highlight that the two intraclasts were formerly continuous. The surface of the intraclasts ranges from rough to smooth and may be locally covered by micritic laminar calcretes (Figure 7K). Between intraclasts, the filling consists either of gastropods and reworked polygenetic carbonate intraclasts within a micritic matrix that is rarely desiccated or by sparite cements (Figure 7J,K,L). The alternation of mudstone and wackestone with root traces (facies F5h) exhibits a palustrine carbonate in the upper part of the beds, while the bottom is unaffected by subaerial exposure (Figure 7N). Peloidal grainstone F5e fills desiccation cracks, microcavities or karstic channels within previously described facies.

Oxygen and carbon isotopes—The isotope compositions are depleted in ^{13}C and ^{18}O with values ranging from -8.8 to -4.7‰ for the $\delta^{13}\text{C}$ and from -6.2 to -2.5‰ for the $\delta^{18}\text{O}$ (mean values of -7.1 and -4.6‰ , respectively; Figure 5). The highly negative $\delta^{13}\text{C}$ and $\delta^{18}\text{O}$ values indicate the influence of meteoric fluids (Talbot, 1990). Note however that the micrite of these facies has been modified early by biological activity.

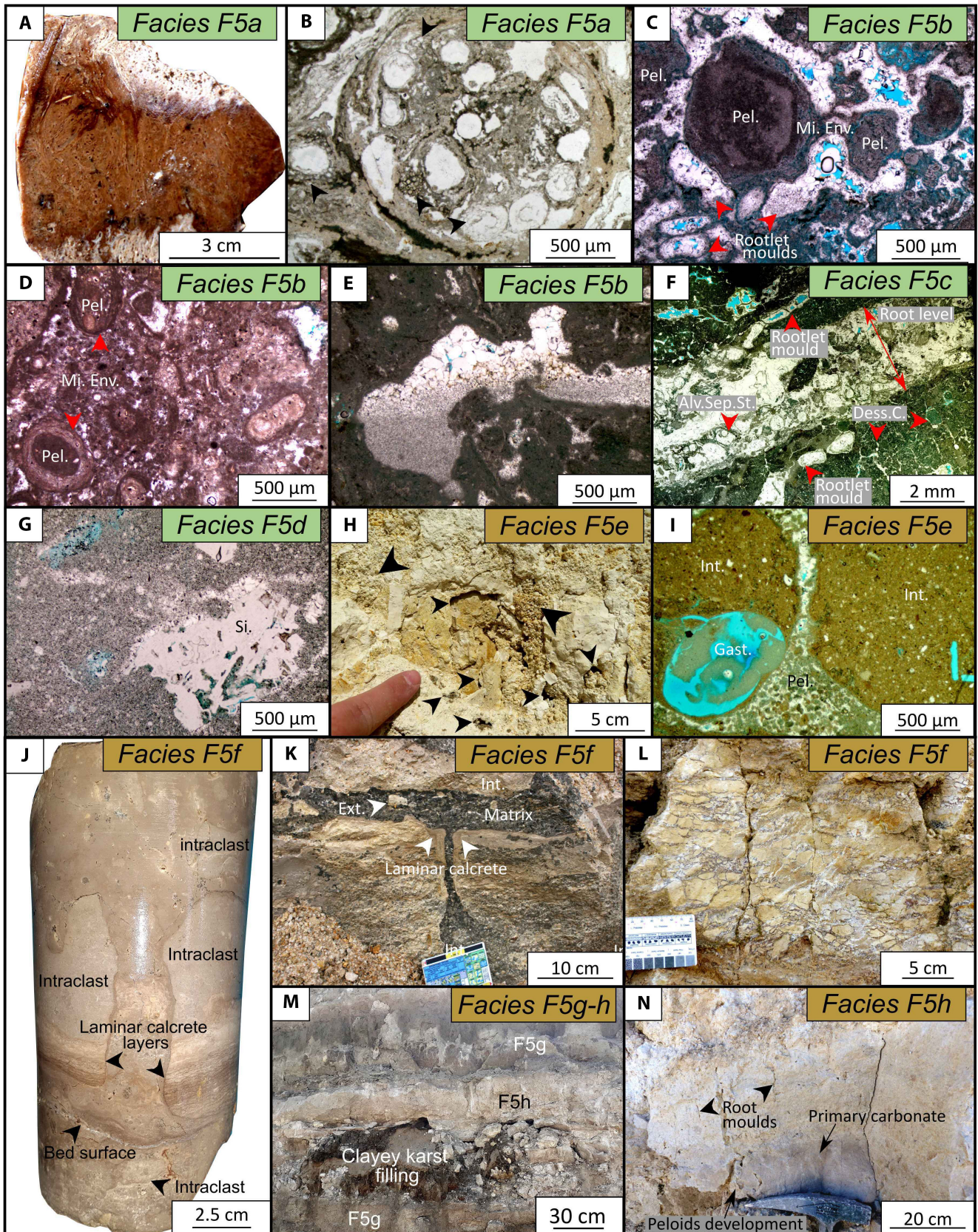
Synthesis—All facies of this facies association FA5 present characteristics of subaerial exposure suggesting the ephemeral presence of water in lacustrine systems or seasonal wetlands, i.e., typical of a palustrine environment (Freytet & Plaziat, 1982; Platt, 1989; Platt & Wright, 1991; Freytet & Verrecchia, 2002; Alonso-Zarza & Wright, 2010a). The muddy limestone represents the highest water level while the subaerial exposure features (peloids, roots, desiccation, ...) record the depositional system with the lowest water level (Freytet & Plaziat, 1982; Platt & Wright, 1991; Bohacs et al., 2000; Freytet & Verrecchia, 2002; Alonso-Zarza & Wright, 2010a). Facies F5a to F5d are interpreted as calcretes composed mainly of beta microfabrics which were formed during long or intense episodes of subaerial exposure (Wright, 1994; Kosir, 2004; Kabanov et al., 2008; Alonso-Zarza & Wright, 2010a). The presence of alveolar-septal structures, rootlet moulds and

FIGURE 6 Coastal lake facies association FA3. The numbers indicated [#] correspond to the location of the boreholes and sedimentary sections in Figure 1. (A) Cores presenting alternating gypsum, limestone and organic matter; Facies F3a; Masses de gypses Formation, Priabonian [28]. (B) Gypsum developing in limestone; Facies F3a; Marnes et Caillasses Formation, Lutetian–Bartonian [1]. (C) Limestone with calcite dendrites and recrystallised gastropods (some are shown with black arrows); Facies F3a; Calcaire de Saint-Ouen Formation, Bartonian [5]. (D) Wackestone with microfossils; Facies F3b; Calcaire de Saint-Ouen Formation, Bartonian [2]. (E) Wackestone with peloids (Pel.), ostracods and small foraminifera (benth. foram.); Facies F3b; Calcaire de Saint-Ouen Formation, Bartonian [7]. (F) Shell-rich packstone with ostracods, charophytes, gastropods (gastr.) and euryhaline benthic foraminifera (benth. foram.); Facies F3c; Calcaire de Saint-Ouen Formation, Bartonian [6].



Microcodium in these facies, plus fenestral fabrics in some layers in facies F5c suggest a rhizogenic origin (Wright et al., 1988; Wright, 1989; Alonso-Zarza, 1999;

Alonso-Zarza & Wright, 2010). These facies record the strong weathering of the primary carbonate of the Lutetian, Priabonian, Rupelian and Aquitanian.



4.6 | Facies association FA6 Inland lake

Petrography and sedimentary structures—This association is composed of seven facies: (1) polygenetic breccia (facies

F6a), (2) wackestone with lithoclasts (facies F6b), (3) grainstone with peloids and shell fragments (facies F6c), (4) shell-rich floatstone (facies F6d), (5) oncoidal wackestone to packstone (facies F6e), (6) microbial crust (facies

FIGURE 7 Palustrine carbonate facies association FA5. The numbers indicated [#] correspond to the location of the boreholes and sedimentary sections in [Figure 1](#). (A and B) Rhizoliths. Root cells are still identifiable (black arrows). Rootlet moulds are filled by calcedony (in white); Facies F5a; Calcaire de Beauce Formation, Aquitanian [12]. (C and D) Peloids coated by micritic envelopes (mi.env); Facies F5b; Calcaire de Champigny Formation, Priabonian [18 and 21]. (E) Geopetal cement in nodular brecciated limestone; Facies F5b; Calcaire de Champigny Formation, Priabonian [8]. (F) Laminar brecciated limestone displaying a recrystallised millimetre-thick root level with alveolar septal structures (Al. Sep. St.) around which desiccation cracks (Dess.C.) develop; Facies F5c; Calcaire de Brie Formation, Rupelian [8]. (G) Chalky altered limestone with recrystallised micrite in microsparite and silica (Si.); Facies F5d; Calcaire de Champigny Formation, Priabonian [8]. (H) Peloidal grainstone (large arrows) filling a karstic cavity (small arrows); Facies F5e; Calcaire d'Etampes Formation, Rupelian [8]. (I) Peloidal grainstone (facies F5e) filling spaces between two *in-situ* intraclasts with gastropods (gast.); Facies F5e and F5f; Calcaire de Beauce Formation, Aquitanian [16]. (J) *In-situ* brecciated limestones with stromatolitic-like structures inside the intraclasts; Facies F5f; Calcaire de Beauce Formation, Aquitanian [14]. (K) *In-situ* brecciated limestones with a thin layer of laminar calcrete visible around the *in-situ* intraclasts; Facies F5f; Calcaire de Beauce Formation, Aquitanian [16]. (L) *In-situ* brecciated limestones showing jigsaw-puzzle like centimetre-sized intraclasts marking desiccation of the former carbonate rock. The intergranular space is cemented with vadose and phreatic cements; Facies F5f; Calcaire de Provins Formation, Lutetian [18]. (M) Alternation of palustrine facies F5g and F5h affected by the development of a metre-sized karstic cavity; Calcaire de Beauce Formation; Aquitanian [11]. (N) Wackestone with root traces and peloid development; Facies F5h; Calcaire d'Etampes Formation, Rupelian [8].

F6f), and (7) alternations of mudstone and marls (facies F6g; [Figure 8](#)). Gastropods are the main fossil found in these facies; ostracods and charophytes are present in lesser amounts. Fenestral porosity is present and filled by dogtooth or drusy sparite cements. Polygenetic breccia facies (F6a) display reworked carbonate intraclasts of a few centimetres to a few tens of centimetres in size with different morphologies (rounded to sub-angular) and origins (black pebbles, microbial crusts, palustrine carbonate) without preferential orientation, and locally attesting to a polyphase process of breccia formation ([Figure 8A,B](#)). Lithoclastic wackestones (facies F6b) exhibit similar reworked intraclasts but with smaller millimetre-sized fragments and lower proportions of grains. The clasts are mostly rounded and sometimes concentrated along horizontal levels a few millimetres thick ([Figure 8C](#)). Within centimetre-thick to decimetre-thick grey to bluish indurated beds, floatstones and rudstones with gastropods (F6d) or with oncoids (F6e) are present ([Figure 8E,F,G](#)). Desiccation is often identified at the top of the beds. Alternation of clear and dark millimetre-thick micritic laminae, with the dark ones occasionally containing some fragments of organic matter can form columnar or planar structures covering exposure surfaces or filling the intergranular space ([Figure 8H](#)). Encrusted shells (Lymnaeidae) are unaltered and intact when in contact with the laminae. These laminae are interpreted as microbial crusts (facies F6f). They display often micritic and rarely hybrid laminated microfabrics (Vennin et al., 2021). Finally, the mudstone-marl alternation (facies F6g) is composed of beds of mudstones or wackestones several centimetres thick with reworked intraclasts and gastropods alternating with marls ([Figure 8I](#)). No subaerial exposure features were identified in this facies.

Oxygen and carbon isotopes—The isotopic values of these facies are negative, ranging from -7.8 to -4.3% for the $\delta^{13}\text{C}$ and from -4.8 to -2.3% for the $\delta^{18}\text{O}$, and a

covariation is identified (mean values of -6.8 and -3.2% , respectively; [Figure 5](#)). These values correspond to the range found in modern temperate lakes and confirm the formation of the micrite in meteoric water (Talbot, 1990).

Synthesis—The biota and isotope composition of the micrite of this association indicates deposition in a fresh to brackish-water lake, isolated from any marine influence. “Pure” lacustrine limestones are rare, with most showing slight signs of subaerial exposure towards the top of the beds (desiccation cracks, tubular voids interpreted as rootlet moulds, fenestral porosity). The polyphasic breccia indicate multiple reworking of the sediment ([Figure 8B](#)). Black lithoclasts present in these breccia (facies F6a), known as “black pebbles” (Platt, 1989), attest to a short transport distance from the palustrine system (Platt, 1989; Miller et al., 2013). Because such breccia generally occur above subaerial exposure surfaces, they are interpreted as resulting from reworking of primary sediment in shallow water. The facies F6b is interpreted as resulting from deposition of the smallest reworked intraclasts transported over longer distances than that seen in facies F6a formed. In the mud–wackestone and clayey marl alternations (facies F6g) ([Figure 8I](#)), the absence of subaerial features and organic matter-rich or clayey levels suggests a deposit far from the lake margins but still above the hypolimnion (Platt & Wright, 1991; Gierlowski-Kordesch, 2010). This facies association is encountered in the last episodes of carbonate sedimentation in the Paris Basin in the Calcaire d'Etampes (late Rupelian) and the Calcaire de Beauce (Aquitanian) formations.

5 | STRATIGRAPHIC SEQUENCES, FACIES DISTRIBUTION AND PALAEOENVIRONMENTAL EVOLUTION

The two cross-sections are constructed above and below the major subaerial unconformity R2, which is taken as



a horizontal surface (Figures 9 and 10). This precedes the marine transgression of the Sables de Fontainebleau Formation above palustrine or lacustrine formations (Calcaire de Brie and Caillasses d'Orgemont formations).

The stratigraphic surfaces defined by Briais (2015) were correlated further south and east in the lacustrine and palustrine facies and help to define cycles. Fifteen short-term stratigraphic cycles (shorter than 4 Myrs long)

FIGURE 8 Inland lake facies association FA6. The numbers indicated [#] correspond to the location of the boreholes and sedimentary sections in [Figure 1](#). (A) Polygenetic breccia with black angular limestone pebbles and reworked carbonate intraclasts; Facies F6a; Calcaire de Beauce Formation, Aquitanian [16]. (B) Polyphase and polygenetic limestone breccia; Facies F6a; Calcaire de Beauce Formation, Aquitanian [14]. (C) Reworked limestone intraclasts forming beds in a micritic matrix; Facies F6b; Calcaire de Beauce Formation, Aquitanian [14]. (D) Grainstone with peloids and shell fragments (red arrows); Facies F6c; Calcaire de Beauce Formation, Aquitanian [12]. (E and F) Gastropod (gast.)-rich rudstone beds. An erosional surface separates facies F6d from facies F6e in picture F; Facies F6d; Calcaire de Beauce Formation, Aquitanian [13]. (G) Beds of oncoidal rudstone; Facies F6e; Calcaire de Beauce Formation, Aquitanian [13]. (H) Columnar laminated microbial crusts overlying an eroded surface; Facies F6f; Calcaire de Beauce Formation; Aquitanian [16]. (I) Alternating mudstones and gastropod marls; Facies F6g; Calcaire d'Etampes Formation, Rupelian [10].

have been identified from the Lutetian to the Rupelian (47–28 Ma) using the facies associations described above. The average duration of a cycle is approximately 1.25 Myr, which matches the range of duration of third-order cycles (Vail et al., 1991; Hardenbol et al., 1999). All these cycles are included in four lower-order cycles (longer than 4 Myrs long), considered by Briais (2015) as second-order cycles. The first one ranges from the Lutetian to the early Bartonian (LB cycle, duration ≈ 7 Myr) and is delimited by the L1 and B2 subaerial unconformity. It is followed by the early Bartonian to middle Priabonian (BP cycle, ≈ 7 Myr) and the middle Priabonian to late Rupelian (PO cycle, ≈ 7 –8 Myr) cycles topped, respectively, by the P3 and A1 subaerial unconformity. The final cycle ranges from the Aquitanian to the Burdigalian (A cycle, ≈ 4 –5 Myr). These cycles are detailed below.

5.1 | Lutetian– early Bartonian LB cycle: Isolation of the marine carbonate platform

The Lutetian to early Bartonian LB cycle contains three short-term cycles (LB1, LB2 and LB3), each one mainly composed of marine carbonate rocks from the FA1 and FA2 facies associations. This cycle extends from the erosional subaerial unconformity L1, recording a 2 Myrs long hiatus (Pomerol, 1989; Briais et al., 2016), to the erosional subaerial unconformity B2 at the top of the Marnes et Caillasses Formation. The deposits thin out from north to south ([Figure 9](#)). Biostratigraphic data and sequence stratigraphic correlations suggest that the maximum flooding surfaces of each cycle, L2, L3 and B1, are onlapping southwards and westwards ([Figures 9 and 10](#)). The Lutetian marks a long-term regression from open marine (facies association FA1) to restricted marine environments (facies association FA2). Nonetheless, the maximum flooding surfaces L2 and L3 seem to not extend beyond the Remarde Anticline ([Figure 9](#)) and Melun ([Figure 10](#)), where they merge with the L1 surface, while the B1 maximum flooding surface stretches further southwards and westwards to Pithiviers and Etampes ([Figures 9 and 10](#)).

Biota suggest that, during the LB1 and LB2 cycles, the deepest bathymetries were located in the northern part of the basin, decreasing southwards and along the Bray and Remarde anticlines (Merle, 2008). The upper regressive systems tract of the LB2 cycle records the shallowing of the basin with the appearance of restricted marine limestones (FA2), which persists throughout the LB3 cycle with several evaporitic episodes around Paris ([Figures 9 and 11B](#)). Restricted marine deposits pass laterally into a palustrine domain extending westwards to Provins ([Figures 10 and 11B](#)) with *in-situ* brecciated limestones (facies F5f, Calcaire de Provins Formation) and southwards from Pithiviers to Orléans with several facies displaying the freshwater gastropod *Biomphalaria pseudoammonia* (facies F5f, F5g, F5h; Turland, 1974; Mégnien, 1980; Gély & Lorenz, 1991; Merle, 2008).

5.2 | Early Bartonian to middle Priabonian BP cycle: from an estuarine to a carbonate-evaporitic lacustrine system

The long-term BP cycle records six short-term cycles (BP1 to BP6), marking a marine transgression above the Marnes et Caillasses Formation (subaerial unconformity B2) during the early Bartonian with estuarine and tidal siliciclastic sands (BP1 to BP3; Briais, 2015), and then isolation of the basin during the late Bartonian to middle Priabonian with lacustrine and evaporitic deposits (facies association F3, BP4 to BP6) ([Figures 9 and 10](#)). The cycle ends with the subaerial unconformity P3 at the top of the Marnes et Masses de gypses and the Calcaire de Champigny formations.

The first three short-term cycles (BP1 to BP3) present the same geometries as the Lutetian cycles LB1 and LB2, i.e., a maximum thickness and depth in the northern part of the basin and thinning southwards where the maximum flooding surfaces are interpreted to onlap and facies are shallower ([Figure 9](#)). A sedimentary hiatus is identified in the eastern part during these cycles ([Figure 10](#)). During the last three short-term cycles of the BP cycle (BP4 to

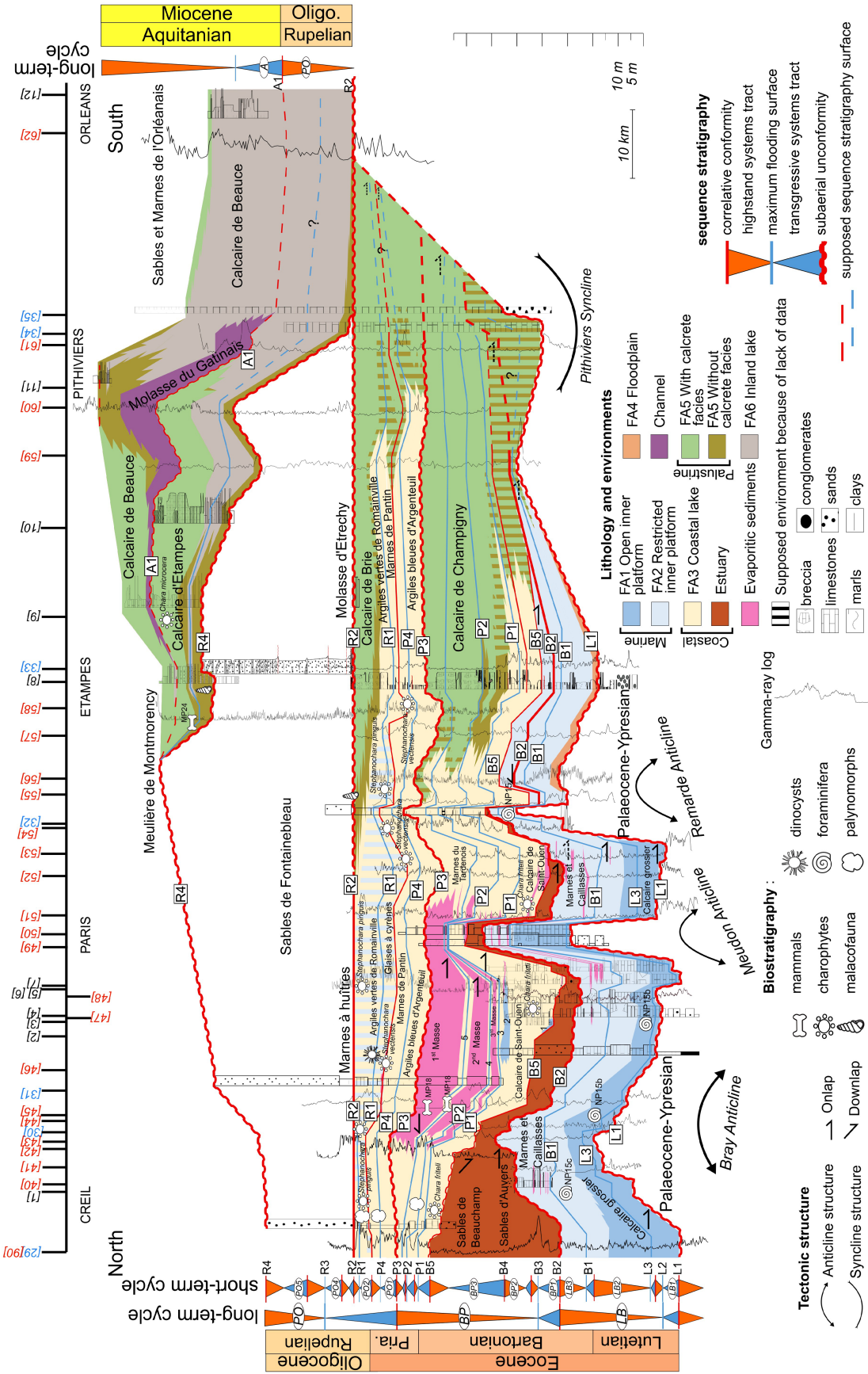


FIGURE 9 Correlation diagram of Lutetian to Miocene sections along a north–south transect between the Mont-Pagnotte borehole and Orléans. This diagram incorporates 12 outcrop sections examined in this study supplemented by two sections from the literature and 28 boreholes. Correlations are based on biostratigraphy (foraminifera, mammals, dinocysts, charophytes, malacofauna and palynomorphs; Cavelier, 1968; Le Calvez, 1970; Pomerol & Riveline, 1975; Aubry et al., 1977; Riveline, 1983) and the definition of 16 stratigraphic cycles delimited by subaerial unconformities and their correlative conformities. The names of the localities associated with the numbers indicated [#] are in Figure 1D. The facies architecture is not described for the Sables de Fontainebleau Formation. 1: Sables de Mortefontaine; 2: Sables de Cresnes-Monceau; 3: Marnes à lucines; 4: Marnes à lucines; 5: Marnes d'entre-deux-Masses.

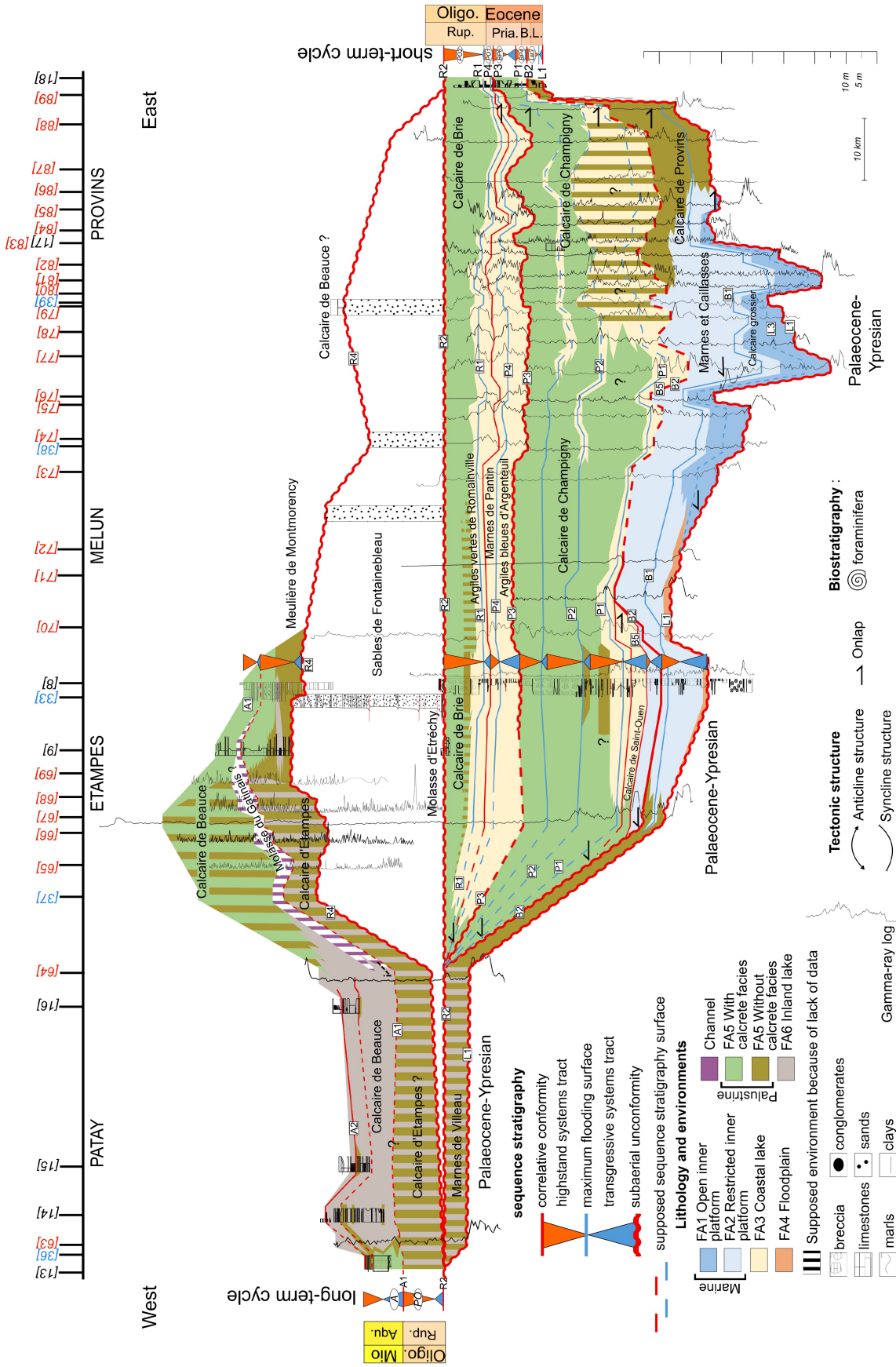


FIGURE 10 Correlation diagram of Lutetian to Miocene sections along an east–west transect between La Baronnie quarry and Les Grands Réages quarry. This diagram incorporates eight outcrop sections examined in this study supplemented by three sections from the literature and 29 boreholes. Correlations are based on the definition of nine stratigraphic cycles delimited by subaerial unconformities and their correlative conformities at Maisse. The names of the localities associated with the numbers indicated [#] are in [Figure 1D](#).

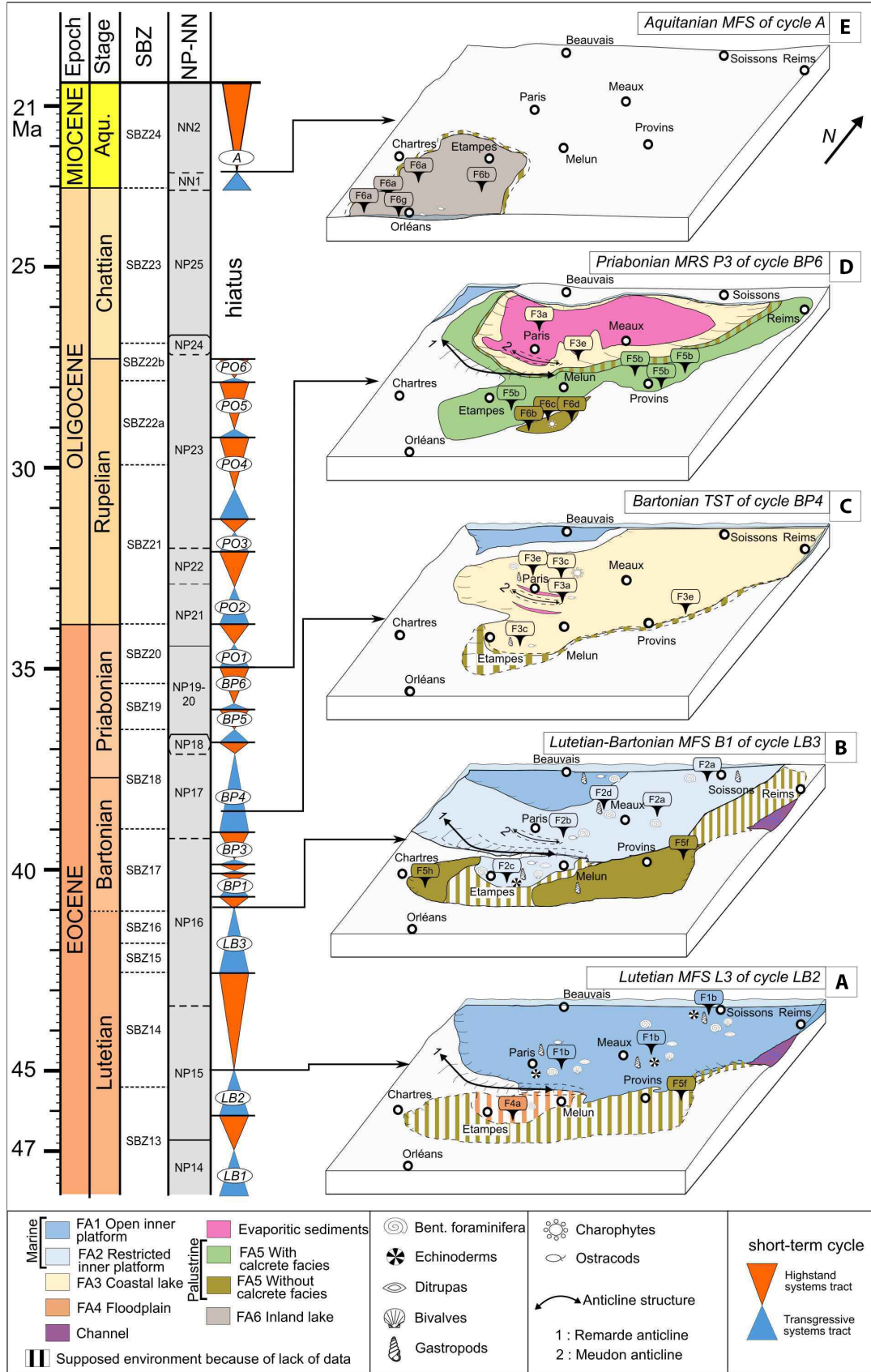


FIGURE 11 Palaeoenvironmental evolution during five periods of carbonate sedimentation. These reconstructions are based on the cross-sections of this study (Figures 9 and 10) and on pre-existing palaeoenvironmental maps (Mégnién, 1980; Merle, 2008; Briais, 2015). The Shallow Benthic Zone (SBZ) and the Calcareous Nannofossils (NP) are based on the global chronostratigraphic chart (Speijer et al., 2020).

BP6), lacustrine limestones, marls and evaporites develop from Creil to Etampes (FA3, Calcaire de Saint-Ouen to the top of Marnes et Masses de gypses formations), passing southwards and eastwards into palustrine limestones (FA5, Calcaire de Champigny Formation, [Figures 9 and 11C,D](#)). The maximum thickness of deposits occurs in Paris and decreases northwards. Deposits also thin out around the Meudon and Remarde anticlines ([Figure 9](#)). At Paris, the transgressive systems tract of the BP4 cycle is composed of lacustrine marl and limestone facies mixed with thin evaporite layers while it thins out completely eastwards (facies F3a-d; Calcaire de Saint-Ouen Formation; [Figures 9 and 10](#)). The maximum flooding surfaces of cycles BP4 to BP6 are identified as gypsiferous marls (facies F3e) with marine or brackish fauna (respectively inside the Marnes à *Pholadomya ludensis* Member for BP4, Marnes à lucines Member for BP5, and Marnes d'entre-deux-Masses Member for BP6). Episodes of connection with marine water are marked by the occurrence of marine bivalves or foraminifera along the maximum flooding surfaces (Pomerol et al., 1965; Mégnien, 1980), which record salinity close to but lower than that of normal seawater. The highstand systems tracts of cycles BP4, BP5 and BP6 correspond to gypsum deposits around Paris, and spread as far as the Meudon Anticline as noted by Gély & Lorenz (1991) and Mégnien (1974). From the BP4 to BP6 cycles, a palustrine domain dominated by calcretes (F5a to F5d) migrates from Pithiviers, Melun and Provins towards Paris ([Figures 9, 10 and 11D](#)). Along the margins of the basin, palustrine sequences presenting coastal lacustrine facies FA3, *in-situ* brecciated limestones F5f or chalky altered limestones F5d overlaid by other calcretes (facies F5a-c) develop in several locations [8, 17 and 20 in [Figures 1D, 10 and 12](#)]. Maximum flooding surfaces of each cycle are located inside the less modified beds by pedogenetic processes, mainly in limestone and marl beds containing ostracods, charophytes and foraminifera (facies F3b, F5f or F5g; [Figure 12](#)).

The descriptions in the west and north-west of the basin of the same palustrine limestones as in the south and south-east (Mégnien, 1980) and the thinning of sediments in the north of the basin ([Figure 9](#)) suggest that the lake was periodically closed to the marine domain and surrounded by a frequently exposed palustrine area ([Figure 11D](#)).

5.3 | Middle Priabonian to early Rupelian PO cycle: from coastal lakes to inland lakes

The long-term PO cycle is composed of six short-term cycles (PO1 to PO6) showing the evolution of a lacustrine

domain (facies association FA3) into a sandy marine environment. The PO cycle ends with the establishment of lacustrine and palustrine domains (F5 and F6) in the southern part of the basin. It ends with the subaerial unconformity A1, corresponding to a major sedimentary hiatus beginning at the end of the Rupelian and extending throughout the Chattian ([Figure 9](#)). In some localities between Etampes and Orléans, this hiatus is located between the Calcaire d'Etampes (Rupelian) and the Molasse du Gatinais (Aquitanian) formations with sandy or silty marl levels directly overlying lacustrine carbonates. Depocentres are located around Paris until the last short-term cycle PO6, when the depocentre migrates southward.

During the PO1 and PO2 cycles, gypsiferous marls (facies F3e, Argiles bleues d'Argenteuil, Marnes de Pantin, Glaises à cyrènes and Argiles vertes de Romainville members) displaying brackish to marine fauna develop in a coastal lake environment in the northern part of the basin from Creil to Pithiviers ([Figure 9](#)). They pass southwards and eastwards into palustrine deposits with calcrete facies (facies association FA5, Calcaire de Brie Formation). Palustrine environments migrate strongly northwards during the deposition of the highstand systems tracts of the PO2 sequence ([Figure 9](#)). These cycles exhibit the same facies and sequences as the BP5 and BP6 cycles previously described. The maximum thickness of the PO3, PO4 and PO5 cycles is seen around Paris and Etampes and thins southwards and eastwards with the Sables de Fontainebleau Formation ([Figures 9 and 10](#)). This formation marks a sandy marine transgression from the north-west to the south-east of the basin ([Figure 9](#)). Cycle PO6, however, displays a maximum thickness in the south and east of the study area with alternating lacustrine and palustrine facies passing to calcrete facies from Orléans to Etampes (facies F5b, F5c, F5e, F5g, F5h, F6b, F6d, F6f and F6g; Calcaire d'Etampes Formation; [Figure 9](#)). It is correlated with a sedimentary hiatus from Paris to Creil ([Figures 9 and 10](#)).

5.4 | Miocene A cycle, a lake on a low energy microbial asymmetrical lacustrine–palustrine margin

This last long-term cycle corresponds to the Neogene deposits in the Paris Basin and contains the carbonate lacustrine Aquitanian Molasse du Gatinais and Calcaire de Beauce formations and the siliciclastic fluvial Sables et Marnes de l'Orléanais Formation. They occur after a 5 Myr long hiatus covering the Chattian (Pomerol, 1989) throughout the basin ([Figure 11E](#)). The transgressive systems tract of this long-term cycle is composed of lacustrine and palustrine limestones (commonly facies F5f, F5g, F5h,

FIGURE 12 Carbonate section of the Bartonian-Priabonian in the Maise borehole (location 8 in [Figure 1](#)) with the associated gamma-ray log, the vertical facies succession, the interpretation of sediment exposure time to subaerial processes, and the sequence stratigraphic interpretations. Refer to Section 4 for the facies and facies association nomenclature and explanations of their interpretation. Note that the gamma-ray log effectively distinguishes between different facies associations (FA). Abrupt facies changes and erosive surfaces characterise subaerial unconformities.

F6a, F6b, F6d, F6e and F6f) in the north of the Miocene basin (locations 11, 13, 14, 15, 16 and 24 in [Figures 1D, 9, 10 and 11E](#)) and more clayey facies near the depocentre at Orléans (facies F6b, F6c and F6g) ([Figures 9, 10 and 11E](#)). Multiple shorter depositional sequences are topped by desiccation cracks and indicate successive lake-level variations. The last highstand systems tract recorded by a succession of desiccated limestones (facies F6d, F5f and F5h) covered by cryoturbated white marls, with the A2 subaerial unconformity at its top, is identified at the top of the Calcaire de Beauce Formation in several localities in the basin (locations [11], [13], [14], [15] and [16] in [Figures 10 and 13](#)).

Differences in facies on either side of the basin are recognised and record differences in water inflow. Facies F6b is associated with *in-situ* brecciated limestones (facies F5f) along the western margin [locations 13, 14, 15, 16 and 24 in [Figure 1D](#)], and with limestones with root traces and wackestones or marls with lithoclasts (respectively facies F5h and F5g) on the eastern margin [location 11] ([Figure 13](#)). As the asymmetrical lacustrine system model from Arenas and Pardo (1999) suggests, poorly drained margins are more brecciated and subject to the erosion of pre-existing material, while heavily vegetated fringes develop along well-drained margins. Therefore, the Aquitanian lake shows an asymmetrical profile with a poorly drained western margin and a well-drained eastern margin. This scheme is consistent with the presence of a fluvial system arriving from the south-east at the beginning of the A cycle.

6 | DISCUSSION

6.1 | Marine and tectonic influences on palaeoenvironments and sedimentary geometries

Each short-term and long-term cycle was readjusted in time thanks to the biostratigraphic framework detailed in Sections 2 and 3 in three locations: in the centre and the north (locations around Paris [1 to 7] in [Figure 1D](#)), in the south (locations around Maise [8 to 16], and to the east (Provins [17 to 21])). Some uncertainties remain, however, about the exact age of surfaces. Because coastal lacustrine facies show connections

with the marine realm, these cycles are compared to the global sea-level curve and European marine cycles ([Figure 14](#); Hardenbol et al., 1999; Miller et al., 2020; Speijer et al., 2020). The maximum flooding surfaces of the BP4, BP6 and PO1 cycles in the central and northern parts of the study area can be correlated to those in other European basins ([Figure 14](#)). This could indicate that these cycles are being controlled by large-scale sea-level variations. However, it was not possible to identify these cycles in the eastern part of the basin. Only the major regressive trend is recorded ([Figure 14](#)). This indicates that the control of relative sea-level variations over short-order cycles decreased or even disappeared eastwards, where environments lay further from the marine domain. However, the Bartonian-Priabonian short-term cycles of the Paris Basin and of European basins are not consistent with global sea-level variations, which means that these sea-level variations are not principally a result of eustasy. For example, the major unconformity P3 coincides well with a sequence boundary in European cycles but corresponds to a global sea-level maximum ([Figure 14](#)). Moreover, the short-term cycles identified in the Paris Basin during the Lutetian-Bartonian differ somewhat from third-order cycles in other European basins, both in number and age while the study area was mostly occupied by estuarine, restricted or even open marine platform environments during this period ([Figure 14](#); Hardenbol et al., 1999; Speijer et al., 2020). These differences may be explained by local and/or regional tectonic movements (Briais, 2015). When the tectonic constraints relaxed, the palaeotopography flattened, enabling the deposition of marine sediments over long distances, which then represent maximum flooding surfaces. There is no discernible link between the PO6 and A cycles and the eustatic cycle.

The long-term cycles (5–10 Ma) of the Paris Basin do not correlate with those of the European basins. It likely indicates that long-term cycles are mainly controlled by tectonics ([Figure 14](#)). The cross-sections highlight three different basin configurations ([Figures 9, 10 and 14](#)): (1) during the Lutetian and Bartonian, the depocentre was located north of the Bray Fault and deposits progressively overlapped southwards; (2) from the late Bartonian to early Rupelian, the depocentre migrated to Paris and to the eastern part of the basin while the northern part of the basin and the Meudon Anticline underwent uplift; (3) during

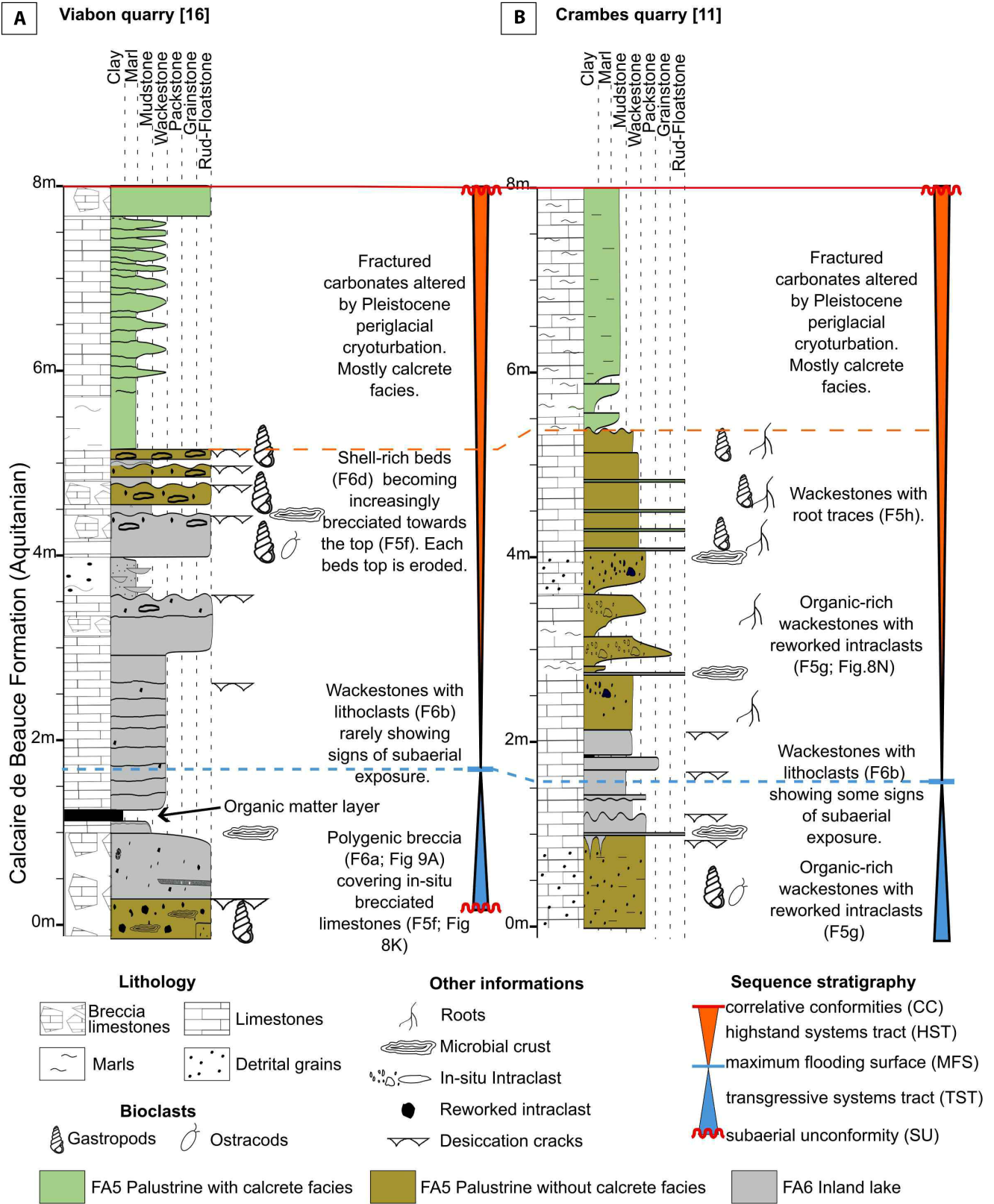


FIGURE 13 Schematic logs of the Viabon (A) and Crambes (B) quarries (respectively locations [16] and [11] on Figure 1D) and their stratigraphic sequences.

the late Rupelian, the depocentre moved further south before the large uplift of the basin during the Chattian. The first and second configurations are associated with

Pyrenean deformations whereas the last configuration is linked to Alpine deformations (Guillocheau et al., 2000; Bourgeois et al., 2007; Briais, 2015). The depocentre

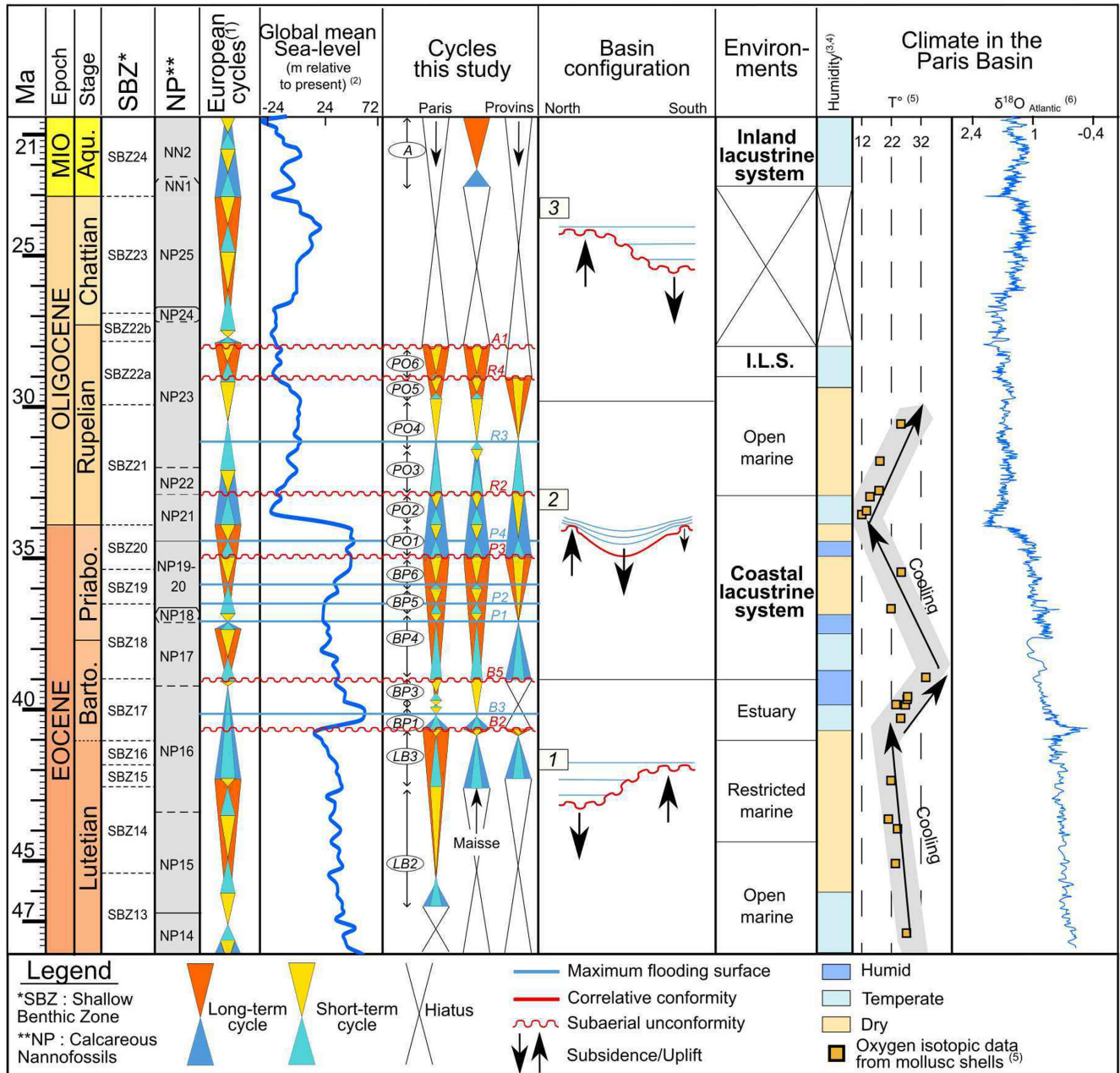


FIGURE 14 Synthetic chronostratigraphic diagram from the Lutetian to the Aquitanian showing stratigraphic cycles in Europe and in the Paris Basin (1: Speijer et al., 2020), global sea-level variations (2: Miller et al., 2020), the evolution of the Paris Basin configuration resulting from tectonic activity and the evolution of depositional systems/environments, and climate (3: Châteauneuf, 1980; 4: Mégnien, 1980; 5: Huyghe et al., 2015; 6: Cramer et al., 2009). The time of each cycle is based on the biostratigraphic fauna discovered in the basin correlated to the global chronostratigraphic chart (see Section 2 for details; Gradstein et al., 2020).

migration and major palaeogeographical changes related to these deformations resulted in different sedimentary profiles. The first configuration favours the northward connection of the basin to the marine domain, and then the deposition of open and restricted marine facies (associations FA1 and FA2; Calcaire grossier and Marnes et Caillasses formations). The progressive southward migration of the depocentre during the Bartonian–Priabonian

implies a progressive disconnect of the basin from the marine domain and the deposition of coastal lake facies (association FA3, Calcaire de Saint-Ouen and Marnes et Masses de gypses formations). During the Rupelian, the migration of the depocentre even further south implies a complete disconnect with the marine domain, and thus the formation of an inland lake facies (association FA6, Calcaire d’Etampes and Calcaire de Beauce formations).

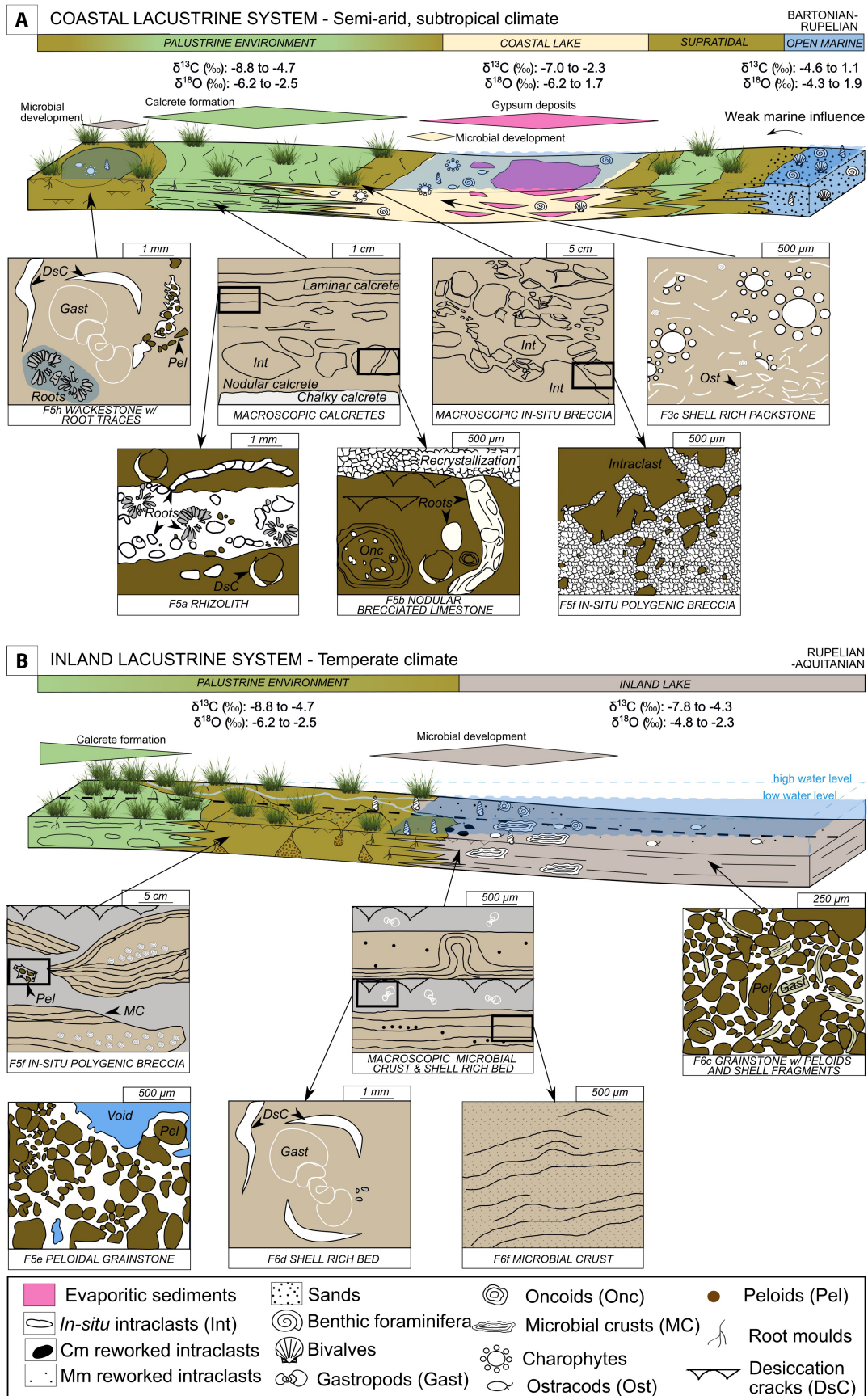


FIGURE 15 Depositional and facies models of lacustrine–palustrine carbonate systems of the Paris Basin during the Cenozoic. (A) Coastal lacustrine system model: mixed carbonate–evaporitic brackish to hypersaline lacustrine to palustrine environments, with episodic connections with the marine domain; semi-arid, subtropical climate; Bartonian to Rupelian. (B) Inland lacustrine system: low energy freshwater microbial lacustrine margin isolated from the marine domain; temperate climate; Rupelian and Aquitanian.

6.2 | Carbonate palaeoenvironment classification at the transition between marine and non-marine domains

It is a challenge to classify and relate facies between marine and non-marine domains in many ancient sedimentary systems especially where outcrops are rare (e.g., the Issirac Basin, France) or with subsurface data (coquina formations in the Campos, Santos or Sergipe basins, Brazil; Thompson et al., 2015; Lett eron et al., 2018; Favoreto et al., 2021). In some previous works focussing on the Cenozoic of the Paris Basin, palaeontologists based their palaeoenvironmental definitions on salinity criteria (Abrard, 1925; Denizot, 1927; Blondeau et al., 1965; Pomerol et al., 1965; Cavelier, 1968; M egnien, 1974; Turland, 1974; Pomerol & Riveline, 1975; Aubry et al., 1977; M egnien, 1980). Indeed, deposits with a palaeontological record suggesting normal marine salinity were defined as open to restricted marine, deposits with a brackish water fauna were classified as coastal brackish lagoonal, and deposits with freshwater to brackish fossils were interpreted as lacustrine. The large-scale cross-sections traced in this study indicate that levels with marine or brackish fauna are correlated with those with brackish to freshwater fauna without any thickness variations and without “barrier” facies (sand bars, palaeosols, marshes etc.). This suggests a salinity gradient within a single waterbody rather than separate lakes or lagoons. These salinity gradients must therefore have resulted from the mixing of seawater and meteoric water from the drainage basin, and/or from a variable evaporation rate. Three distinct settings (restricted marine domain, coastal lake and inland lake) can be defined based on facies, salinity, sedimentary geometries, palaeogeography and carbon and oxygen isotope data of micrites.

First, the restricted marine platform (facies association FA2) was attached to the marine domain, experiencing variable salinity (marine, brackish or hypersaline water) and deposition of marine influenced sediments (diversified marine fauna, slightly negative $\delta^{13}\text{C}$ values). This setting developed in the Paris Basin during Lutetian–early Bartonian times (Figure 11A,B). Second, during Bartonian–Rupelian times the coastal lake (FA3) in the Paris Basin was dominated by meteoric and fluvial waters although ephemeral connections occurred with the marine domain ($\delta^{13}\text{C}$ and $\delta^{18}\text{O}$ values covary and are negative; Figure 11C,D). Finally, the inland lake setting (FA6) is disconnected from any marine influences and freshwater sediments formed (late Rupelian and Aquitanian stages in the Paris Basin; Figure 11E). The following parts of the discussion presents detailed facies models and differences for the newly defined coastal lake and inland lake settings.

6.2.1 | The coastal lacustrine system

The coastal lacustrine system (facies association FA3 and FA5, Figure 15) was dominated by freshwater, recorded in the lacustrine sediments by the abundance of ostracods, charophytes and gastropods, but had ephemeral connections with the marine domain (Figure 15A). Carbon and oxygen isotopes show a large range of values but are lower than those from the restricted marine carbonates (Figure 15A). This indicates variation in salinity due to (1) the mixing between meteoric and marine waters and (2) a decrease in the inflow–evaporation ratio (Figures 5 and 15; Talbot, 1990). Carbonate facies are micritic with some bioclastic levels (both marine and lacustrine fauna). The faunal content and its diversity are generally greater in marine influenced deposits (F ursich, 1993), which present packstone to rudstone textures (facies F3b and F3c) or marly facies (F3e). Freshwater deposits often present mudstone to packstone textures. Ephemeral connections with the marine domain, probably during storms as attested by the presence of tempestites, favour the development of euryhaline foraminifera and marine fauna in brackish to saline waters (Pint et al., 2017; Fritz et al., 2018).

This system developed under two different climates in the Paris Basin: a subtropical climate (wet with contrasted seasons) during the Bartonian and the Rupelian, and a semi-arid climate (dry with strong seasonality) during the Priabonian (Figure 14; Ch ateaufort, 1980). Under a subtropical climate, gypsum precipitation was reduced and micritic facies (facies F3b and F3c) and varves (facies F3d) formed on the margins and in the depocentre of a stratified lake (Figure 15). Under semi-arid conditions, high gypsum-content deposits formed in the depocentre of the lake (facies F3a and F3e) (Priabonian, Figure 15). Planar microbial laminae formed on the lake margins, mostly with gypsum deposits (facies F3a). The same facies distribution was identified depending on the climate in the oligohaline to mesohaline and hypersaline lake models (Eugster & Hardie, 1978; Allen & Collisson, 1986; Bohacs et al., 2000; Lett eron et al., 2022) or in sabkha and non-marine evaporitic environments (Evans et al., 1969; Warren & Kendall, 1985; Shaw et al., 1990; Cooke et al., 1993; Rouchy et al., 1993; Arenas & Pardo, 1999; Bouton et al., 2016). However, it differs with respect to the presence of marine fauna due to marine connections.

Laterally to the lake (facies association FA3), a palustrine domain (FA5) developed, strongly affected by subaerial exposure (Figure 15A). The negative $\delta^{13}\text{C}$ and $\delta^{18}\text{O}$ values indicate the influence of meteoric fluids (Figures 5 and 15). In this palustrine environment, the initial carbonate formed in low saline meteoric water judging from the biota and the negative carbon and oxygen

isotope values of the micrites (Arenas et al., 1997; Alonso-Zarza & Arenas, 2004; Leng & Marshall, 2004; Huerta & Armenteros, 2005; Fischer-Femal & Bowen, 2021). The palustrine domain was greatly extended in a semi-arid climate, which is consistent with the current view of palustrine carbonate formation (Freytet & Plaziat, 1982; Wright & Tucker, 1991; Platt & Wright, 1992; Alonso-Zarza, 2003; Huerta & Armenteros, 2005; Alonso-Zarza & Wright, 2010; Azerêdo et al., 2015). Palustrine facies show varying degrees of modification by subaerial exposure processes, ranging from simple desiccation of the primary mud (facies F5e and f) to total pedogenic overprinting (facies F5a to d). These varied features (desiccation cracks, microkarsts, root traces, calcretes, rhizoconcretions) reveal different durations of exposure to surface processes, directly dependent on the climate. Under subtropical conditions, these features are less developed and the calcrete facies are thinner in metre-thick depositional sequences. The depositional sequences begin at the base with *in-situ* brecciated limestones (facies F5f) and chalky altered limestones (facies F5d) marking high sedimentation rates and moderate pedogenetic processes, i.e., a high lake-water level during a relatively wet period (Figure 12; Alonso-Zarza & Wright, 2010). The common presence of lacustrine facies below palustrine facies within depositional sequences indicates a lacustrine origin for the micrite. Facies F5f and F5d pass upwards into nodular brecciated limestones (facies F5b) and then tubular and laminar brecciated limestones (facies F5a and F5c), which indicate a lower sedimentation rate and formation by intense pedogenesis during longer periods of subaerial exposure (Figure 12). Subaerial exposure increasingly modified palustrine facies with distance from the lake (Figure 15).

6.2.2 | The inland lacustrine system

The inland lacustrine system (facies associations FA6 and FA5) presents no marine influence but instead indicate sedimentation in freshwater ($\delta^{13}\text{C}$ and $\delta^{18}\text{O}$ values covary and are negative during the late Rupelian and Aquitanian; Figure 15B). Fossils such as gastropods, ostracods and charophytes are present but only abundant in specific locations on the lake margins, where they may form coquinas (facies F6d; Gierlowski-Kordes, 2010). These fossil-rich beds alternate with thick microbial crusts (facies F6f) and oncoidal beds (facies F6e). Desiccation in the lacustrine facies is frequent and marks subaerial exposure. The abundance of reworked intraclast facies (F6a and F6b) and grainstones with peloids and shell fragments (facies F6c) highlights the reworking by waves of desiccated carbonates from the palustrine and lacustrine margins (Strasser, 1984; Platt, 1989;

Vera & Jiménez de Cisneros, 1993; Miller et al., 2013). In the deepest part of the lake, alternations of marls and mudstones (facies F6g) form. As mentioned by Platt and Wright (1992), the highly extended palustrine domain indicates that the lacustrine–palustrine system was mainly shallow, as attested by the abundance of desiccated lacustrine facies (facies F6a, b, d and e) and the rarity/absence of deep-water facies. The palustrine domain that developed laterally to the inland lake is different to the palustrine domain associated with the coastal lake. Fewer calcretes formed and they are localised in the areas furthest from the lake (Figure 15). Instead, organic-rich marls and alternating mudstones and wackestones with root traces (facies F5g and F5h) were more frequent along the lake margins. Breccia facies formed *in-situ* by desiccation or by recycling of the pre-existing and early cemented carbonate are also abundant (facies F5f, F6a). This model is similar to those of Freytet and Plaziat (1982), Allen and Collinson (1986), Platt (1989) or Bohacs et al. (2000) when open or balanced-filled lakes have low-energy margins. Nonetheless, it differs by showing a lower detrital input, abundant microbial crusts and reworked intraclasts, and a large variety of palustrine facies. The differences in facies distribution between the coastal and inland lacustrine systems can be explained by the wetter climate during the Rupelian–Aquitanian than during the Priabonian (Figure 15B; Châteauneuf, 1980).

In the inland lake, micrite is still dominant but microbial activity is clearly more important than in coastal lakes, with the abundance of laminated microbial crusts and microbial oncoids (facies F6e and f). These differences in microbial structures between coastal and inland lakes probably result from climate changes. Indeed, microbial structures are more developed during periods of temperate climate (Rupelian and Aquitanian) (Châteauneuf, 1972; Utescher et al., 2000; Scherler et al., 2013). The enhanced development of microbial structures in wet climates during the Aquitanian is already known from other locations in Western Europe (Roche et al., 2018; Arenas-Abad, 2021; Vennin et al., 2021). High precipitation rates may favour microbial activity by bringing nutrients into the lakes.

Palustrine carbonates formed therefore periodically from the late Lutetian to the Aquitanian in the Paris Basin and pass laterally to restricted marine and lacustrine environments (facies associations FA2, FA3 and FA6). In the fossil record, palustrine carbonates have been identified in numerous settings associated with deposits from internal ramps, lagoons, rivers and lakes (Alonso-Zarza & Wright, 2010a). These carbonates are often linked to significant underlying karstic aquifer systems (Platt & Wright, 2023). These aquifers can supply the necessary

CaCO₃ for carbonate formation in marshes through rising groundwaters (“Groundwater Dependent Carbonate Factories” by Platt & Wright, 2023). Therefore, the appearance and development of palustrine carbonates in the fossil record can be interpreted in response to the aquifer level rising due to marine transgression in coastal settings or regional watershed responses to inland basin filling.

In the case studied here, the palustrine and lacustrine carbonates are currently karstified and overlay the karstified Cretaceous chalk aquifer in the eastern and southern parts of the basin. Although no information about the exact age of these karstifications is known, the presence of Burdigalian mammals in the karsts within the Aquitanian Calcaire de Beauce Formation suggests that some of these karsts formed very early after sedimentation, no later than a few million years. Consequently, the chalk aquifer and possibly underlying karstic aquifers within non-marine carbonates may have controlled the water supply in these lacustrine-palustrine environments. While brief marine connections have been identified in the coastal lacustrine system, they are not recorded in the palustrine domain; their contributions may be relatively minor compared to the inputs from the watershed and underlying aquifers. Moreover, the drier climate of Priabonian-early Rupelian times likely contributed to the extensive development of palustrine facies compared to the late Rupelian and the Aquitanian, affecting the water inflow from the watershed and the evaporation rate. The preservation of these palustrine deposits, which can reach thicknesses of 40–50 m in the Calcaire de Champigny Formation, is likely favoured by local subsidence occurring to the east and south of the basin during the Lutetian-Aquitania.

7 | CONCLUSIONS

The petrographic and facies studies of 35 new sedimentary sections coupled with data from the literature for the coastal and continental carbonate formations of the Cenozoic of the Paris Basin allow us to define 32 facies formed in depositional environments ranging from open marine to lacustrine and palustrine. Key short-term and long-term sequence stratigraphic surfaces (maximum flooding and maximum regressive surfaces) were correlated along two large-scale cross-sections to distinguish spatial and temporal facies evolution and depositional geometries. Two facies models are proposed for coastal and inland lacustrine systems, encompassing both the lacustrine and palustrine environments.

Coastal lacustrine systems developed during the Bartonian and Rupelian in the Paris Basin. These lakes had episodic connections with the marine domain. This environment differs from lagoon environments by a

fauna adapted to low salinity conditions (mesohaline to oligohaline), a strong negative carbon and oxygen anomaly of the micrite indicating a major contribution from continental waters and sediment thicknesses reducing towards the marine domain. Facies correspond to varves or evaporites in the depocentre while micritic carbonates with a brackish fauna were deposited on the lake margins. The associated palustrine domain is mainly marked by the formation of calcrete facies presenting different textures (chalky, nodular, laminar and rhizoliths) and showing successive metre-sized shallowing upwards sequences, recording subaerial exposure. *In-situ* brecciated limestones and chalky calcretes are the palustrine facies located closest to the lake margins. Moving away from the lake, they pass into nodular and then into laminated calcretes and rhizoliths. The latter are the most developed palustrine facies in the coastal lake system.

Inland lacustrine systems developed during the Rupelian and the Aquitanian in the Paris Basin. Lakes became disconnected from the marine domain and were home to freshwater fauna. As a result, oxygen and carbon isotope values are highly negative and less variable than in the coastal lake. Microbial crusts with micritic or hybrid laminated microfabrics and oncoids are frequent and attest to intense microbial activity. In the palustrine domain, organic-rich layers, limestones with root traces and peloidal grainstones formed close to the lake margins. They present subaerial exposure features such as rootlet moulds, desiccation cracks and microkarstification, and they are frequently interbedded with lake facies. *In-situ* brecciated limestones and rare calcrete facies reflect a longer exposure time and are located further from the lake margin.

In the intracratonic Paris Basin, large-scale and long-term tectonic processes were the main control of long-term cycles and led to the southward migration of the depocentre. Tectonism was responsible for the changes from dominant marine environments in the Lutetian to coastal lacustrine systems during the Bartonian and then inland lacustrine systems during the Rupelian and Aquitanian by modifying the connection of the basin with the marine domain. Third-order relative sea-level variations recorded in other European basins seem to control short-term cycles in the coastal lacustrine systems (BP4, BP6 and PO1 cycles), but not in the inland systems. As a result, short and long-term sequence stratigraphic surfaces (maximum regressive and maximum flooding surfaces) could be extended from the marine domain to the coastal lacustrine systems, allowing correlation between these two depositional settings. This reinforces the importance of differentiating between coastal and inland lacustrine environments. The impact of climate on non-marine carbonate production was a major feature in the Paris intracratonic basin. In more temperate

to humid climates, lacustrine carbonate production was induced by microbial activity.

Finally, it is highly likely that the presence of aquifers in the Cretaceous chalk and in the lacustrine-palustrine carbonate formations played a significant role in the formation of the palustrine deposits on the surface, by supplying the calcium carbonate necessary for their formation. However, the existence of such aquifers when palustrine carbonates were formed remains to be proven.

ACKNOWLEDGEMENTS

This study was conducted within the framework of the research collaboration agreement 2019-157 between the BRGM (Bureau de Recherches Géologiques et Minières, French Geological Survey) and Université Paris-Saclay. This project was funded by the BRGM through the “Référentiel Géologique de la France” programme and by a doctoral PhD from the French Ministry of Research and Higher Education (2019-105). We thank all the companies that gave us access to their quarries, without which some of this work would not have been possible: a2c-matériaux, Cemex, Eurovia, Fulchiron, Imerys Ceramic France, Lafarge Holcim, SMBP, and Roland and Dadonville quarries. We are also grateful to the SIARCE for allowing us to describe the Maise borehole. Thanks to Chantal Bourdillon (Stratigraphie et biochronologie) for the identification of foraminifera species and to Philippe Blanc (Lithologie Bourgogne) for the high-quality of thin sections. The two reviewers are thanked for their helpful comments, which greatly improved the manuscript, Kishore Selvam and editor Peter Swart for handling the manuscript.

DATA AVAILABILITY STATEMENT

Data used in this research are available in the Supplementary Information associated with the article as well as upon reasonable request from the corresponding author.

ORCID

Kévin Moreau  <https://orcid.org/0000-0001-5165-8740>

REFERENCES

- Abrard, R. (1925) Le Lutétien du Bassin de Paris: Essai de monographie stratigraphique. 3-2. (in French).
- Alimen, H. (1936) Etude sur le Stampien du Bassin de Paris. *Mémoires. Société Géologique de France*, 14, 304 pp. (in French).
- Allan, J.R. & Matthews, R.K. (1982) Isotope signatures associated with early meteoric diagenesis. *Sedimentology*, 29, 797–817. <https://doi.org/10.1111/j.1365-3091.1982.tb00085.x>
- Allen, J.R. (1980) Sand waves: a model of origin and internal structure. *Sedimentary Geology*, 26, 231–281.
- Allen, P.A. & Collinson, J.D. (1986) Lakes. In: *Sedimentary environments and facies*. London: Blackwell Scientific Publications, pp. 63–94.
- Alonso-Zarza, A.M. (1999) Initial stages of laminar calcrete formation by roots: examples from the Neogene of central Spain. *Sedimentary Geology*, 126, 177–191.
- Alonso-Zarza, A.M. (2003) Palaeoenvironmental significance of palustrine carbonates and calcretes in the geological record. *Earth Science Reviews*, 60, 261–298. [https://doi.org/10.1016/S0012-8252\(02\)00106-X](https://doi.org/10.1016/S0012-8252(02)00106-X)
- Alonso-Zarza, A.M. & Arenas, C. (2004) Cenozoic calcretes from the Teruel Graben, Spain: microstructure, stable isotope geochemistry and environmental significance. *Sedimentary Geology*, 167, 91–108. <https://doi.org/10.1016/j.sedgeo.2004.02.001>
- Alonso-Zarza, A.M. & Wright, V.P. (2010a) Chapter 2: palustrine carbonates. In: Alonso-Zarza, A.M. & Tanner, L.H. (Eds.) *Developments in Sedimentology Carbonates in continental settings: facies, environments, and processes*. Amsterdam: Elsevier 61, pp. 103–131. [https://doi.org/10.1016/S0070-4571\(09\)06102-0](https://doi.org/10.1016/S0070-4571(09)06102-0)
- Alonso-Zarza, A.M. & Wright, V.P. (2010) Chapter 5: calcretes. In: Alonso-Zarza, A.M. & Tanner, L.H. (Eds.), *Developments in Sedimentology Carbonates in continental settings: Facies, environments, and processes*, Vol. 61. Elsevier, Amsterdam, pp. 225–267. [https://doi.org/10.1016/S0070-4571\(09\)06105-6](https://doi.org/10.1016/S0070-4571(09)06105-6)
- Alonso-Zarza, A.M., Genise, J.F. & Verde, M. (2011) Sedimentology, diagenesis and ichnology of Cretaceous and Palaeogene calcretes and palustrine carbonates from Uruguay. *Sedimentary Geology*, 236, 45–61.
- Amao, A.O., Kaminski, M.A. & Setoyama, E. (2016) Diversity of foraminifera in a shallow restricted lagoon in Bahrain. *Micropaleontology*, 62, 197–211. <https://doi.org/10.47894/mpal.62.3.01>
- Arenas, C., Casanova, J. & Pardo, G. (1997) Stable-isotope characterization of the Miocene lacustrine systems of Los Monegros (Ebro Basin, Spain): palaeogeographic and palaeoclimatic implications. *Palaeogeography Palaeoclimatology Palaeoecology*, 128, 133–155. [https://doi.org/10.1016/S0031-0182\(96\)00052-1](https://doi.org/10.1016/S0031-0182(96)00052-1)
- Arenas, C. & Pardo, G. (1999) Latest Oligocene–Late Miocene lacustrine systems of the north-central part of the Ebro Basin (Spain): sedimentary facies model and palaeogeographic synthesis. *Palaeogeography Palaeoclimatology Palaeoecology*, 151, 127–148. [https://doi.org/10.1016/S0031-0182\(99\)00025-5](https://doi.org/10.1016/S0031-0182(99)00025-5)
- Arenas-Abad, C. (2021) A multi-scale approach to laminated microbial deposits in non-marine carbonate environments through examples of the Cenozoic, north-east Iberian Peninsula, Spain. *Depositional Record*, 8, 67–101.
- Arribas, M.E., Bustillo, A. & Tsige, M. (2004) Lacustrine chalky carbonates: origin, physical properties and diagenesis (Palaeogene of the Madrid Basin, Spain). *Sedimentary Geology*, 166, 335–351. <https://doi.org/10.1016/j.sedgeo.2004.01.012>
- Assayag, N., Rivé, K., Ader, M., Jézéquel, D. & Agrinier, P. (2006) Improved method for isotopic and quantitative analysis of dissolved inorganic carbon in natural water samples. *Rapid Communications in Mass Spectrometry*, 20, 2243–2251. <https://doi.org/10.1002/rcm.2585>
- Aubry, M.-P., Blondeau, A., Cavelier, C., Damotte, R., Gruas-Cavagnetto, C., Le Calvez, Y., Odin, G., Pomerol, C., Renard, M., Riveline, J. & Tourenq, J. (1977) Le Paléogène dans le sondage du Mont Pagnotte. *Bulletin d'Information des Géologues du Bassin de Paris*, 14, 3–50 (in French with English abstract).

- Aubry, M.-P. (1985) Northwestern European Paleogene magnetostratigraphy, biostratigraphy, and paleogeography: calcareous nannofossil evidence. *Geology*, 13, 198. [https://doi.org/10.1130/0091-7613\(1985\)13<198:NEPMB>2.0.CO;2](https://doi.org/10.1130/0091-7613(1985)13<198:NEPMB>2.0.CO;2)
- Azerêdo, A.C., Paul Wright, V.P., Mendonça-Filho, J., Cristina Cabral, M. & Duarte, L.V. (2015) Deciphering the history of hydrologic and climatic changes on carbonate lowstand surfaces: calcrete and organic-matter/evaporite facies association on a palimpsest Middle Jurassic landscape from Portugal. *Sedimentary Geology*, 323, 66–91. <https://doi.org/10.1016/j.sedgeo.2015.04.012>
- Blondeau, A., Cavelier, C., Feugueur, L. & Pomerol, C. (1965) Stratigraphie du Paléogène du bassin de Paris en relation avec les bassins avoisinants. *Bulletin de la Société Géologique de France*, 7, 200–221 (in French). <https://doi.org/10.2113/gssgfbull.S7-VII.2.200>
- Bohacs, K.M., Carroll, A.R., Neal, J.E., Mankiewicz, P.J., Gierlowski-Kordesch, E.H. & Kelts, K.R. (2000) Lake-Basin type, source potential, and hydrocarbon character: an integrated sequence-stratigraphic-geochemical framework. *Lake Basins through Space and Time. AAPG Studies in Geology*, 46, 3–34.
- Bohacs, K.M., Grabowski, G., Jr. & Carroll, A.R. (2007) Lithofacies architecture and variations in expression of sequence stratigraphy within representative intervals of the Green River Formation, Greater Green River Basin, Wyoming and Colorado. *Mountain Geologist*, 44, 39–60.
- Bourgeois, O., Ford, M., Diraison, M., de Veslud, C.L.C., Gerbault, M., Pik, R., Ruby, N. & Bonnet, S. (2007) Separation of rifting and lithospheric folding signatures in the NW-Alpine foreland. *International Journal of Earth Sciences*, 96, 1003–1031. <https://doi.org/10.1007/s00531-007-0202-2>
- Bouton, A., Vennin, E., Pace, A., Bourillot, R., Dupraz, C., Thomazo, C., Brayard, A., Désaubliaux, G. & Visscher, P.T. (2016) External controls on the distribution, fabrics and mineralization of modern microbial mats in a coastal hypersaline lagoon, Cayo Coco (Cuba). *Sedimentology*, 63, 972–1016. <https://doi.org/10.1111/sed.12246>
- Brasier, A.T. (2011) Searching for travertines, calcretes and speleothems in deep time: Processes, appearances, predictions and the impact of plants. *Earth Science Reviews*, 104, 213–239. <https://doi.org/10.1016/j.earscirev.2010.10.007>
- Briaux, J. (2015) Le Cénozoïque du bassin de Paris: un enregistrement sédimentaire haute résolution des déformations lithosphériques en régime de faible subsidence. PhD thesis, Université de Rennes, Rennes, 450 pp (in French).
- Briaux, J., Guillocheau, F., Lasseur, E., Robin, C., Châteauneuf, J.J. & Serrano, O. (2016) Response of a low-subsiding intracratonic basin to long wavelength deformations: the Palaeocene–Early Eocene period in the Paris Basin. *Solid Earth*, 7, 205–228. <https://doi.org/10.5194/se-7-205-2016>
- Capezzuoli, E., Della-Porta, G., Rogerson, M. & Tagliasacchi, E. (2022) Non-marine carbonate: wherefore art thou? *Depositional Record*, 8, 4–8. <https://doi.org/10.1002/dep2.170>
- Cavelier, C. (1968) Le Paléogène des forages de Marcoussis (Essonne). *Mémoires. Bureau de Recherches Géologique et Minières (France)*, 58, 389–400 (in French).
- Cavelier, C. (1969) La limite Eocène-Oligocène, Bur. Rech. Géol. Min. Mém., Presented at the Colloque sur l'Eocène, Paris, 431–437 pp. (in French with English abstract).
- Changsong, L., Eriksson, K., Sitan, L., Yongxian, W., Jianye, R. & Yanmei, Z. (2001) Sequence architecture, depositional systems, and controls on development of lacustrine basin fills in part of the Erlian basin, northeast China. *AAPG Bulletin*, 85, 2017–2043. <https://doi.org/10.1306/8626D0DB-173B-11D7-8645000102C1865D>
- Châteauneuf, J.J. (1972) Contribution à l'étude de l'Aquitainien. La coupe de Carry-le-Rouet (Bouches-du-Rhône, France). Ve Congrès du Néogène méditerranéen. Volume III, Étude palynologique. *Bulletin du Bureau de Recherches Géologiques et Minières*, 4, 59–65 (in French).
- Châteauneuf, J.-J. (1980) Palynostratigraphie et paléoclimatologie de l'Eocène supérieur et de l'Oligocène du Bassin de Paris, PhD thesis, BRGM, Paris, 361 pp (in French).
- Cooke, R.U., Warren, A. & Goudie, A.S. (1993) *Desert geomorphology*. London: CRC Press, p. 534. <https://doi.org/10.1201/b12557>
- Copetake, P., Sims, A.P., Crittenden, S., Hamar, G.P., Ineson, J.R., Rose, P.T., Tringham, M.E., Evans, D., Graham, C. & Armour, A. (2003) *The millennium atlas: petroleum geology of the central and northern North Sea*. Bath: Geological Society of London, p. 389.
- Cramer, B.S., Toggweiler, J.R., Wright, J.D., Katz, M.E. & Miller, K.G. (2009) Ocean overturning since the Late Cretaceous: inferences from a new benthic foraminiferal isotope compilation. *Paleoceanography and Paleoclimatology*, 24, 14.
- De Boever, E., Brasier, A.T., Foubert, A. & Kele, S. (2017) What do we really know about early diagenesis of non-marine carbonates? *Sedimentary Geology*, 361, 25–51. <https://doi.org/10.1016/j.sedgeo.2017.09.011>
- Delhaye-Prat, V., Cassagne, B., Guillocheau, F. & Rubino, J.-L. (2005) Sedimentologie des Sables de Fontainebleau et architecture des dépôts oligocènes du Bassin de Paris. *Association des Sédimentologues Français*, 4, 129 pp (in French).
- Della Porta, G. (2015) Carbonate build-ups in lacustrine, hydrothermal and fluvial settings: comparing depositional geometry, fabric types and geochemical signature. *Geological Society of London, Special Publication*, 418, 17–68. <https://doi.org/10.1144/SP418.4>
- Denizot, G. (1927) Les formations continentales de la région orléanaise, PhD thesis, BRGM, Paris, 575 pp (in French).
- Deschamps, R., Rohais, S., Hamon, Y. & Gasparrini, M. (2020) Dynamic of a lacustrine sedimentary system during late rifting at the Cretaceous–Palaeocene transition: Example of the Yacoraite Formation, Salta Basin, Argentina. *Depositional Record*, 6, 490–523. <https://doi.org/10.1002/dep2.116>
- Dunham, R.J. (1962) Classification of carbonate rocks according to depositional textures. *AAPG Memoir*, 1, 108–121.
- Dye, A.H. & Barros, F. (2005) Spatial patterns in meiobenthic assemblages in intermittently open/closed coastal lakes in New South Wales, Australia. *Estuarine, Coastal and Shelf Science*, 62, 575–593. <https://doi.org/10.1016/j.ecss.2004.08.022>
- Embry, A.F. & Klovan, J.E. (1971) A late Devonian reef tract on north-eastern Banks Island, NWT. *Bulletin of Canadian Petroleum Geology*, 19, 730–781.
- Eugster, H.P. & Hardie, L.A. (1978) Chapter 8: saline lakes. In: Lerman, A. (Ed.) *Lakes*. Berlin Heidelberg, New-York: Springer-Verlag, pp. 237–293.
- Evans, G., Schmidt, V., Bush, P. & Nelson, H. (1969) Stratigraphy and geologic history of the Sabkha, Abu Dhabi, Persian Gulf. *Sedimentology*, 12, 145–159. <https://doi.org/10.1111/j.1365-3091.1969.tb00167.x>
- Favoreto, J., Valle, B., Borghi, L., Dal' Bó, P.F., Mendes, M., Arena, M., Santos, J., Santos, H., Ribeiro, C. & Coelho, P. (2021) Depositional controls on lacustrine coquinas from an Early

- Cretaceous rift lake: Morro do Chaves Formation, Northeast Brazil. *Marine and Petroleum Geology*, 124, 104852. <https://doi.org/10.1016/j.marpetgeo.2020.104852>
- Fischer-Femal, B.J. & Bowen, G.J. (2021) Coupled carbon and oxygen isotope model for pedogenic carbonates. *Geochimica et Cosmochimica Acta*, 294, 126–144. <https://doi.org/10.1016/j.gca.2020.10.022>
- Flügel, E. & Munnecke, A. (2010) *Microfacies of carbonate rocks: analysis, interpretation and application*. Berlin: Springer, p. 2004.
- Freytet, P. & Plaziat, J.-C. (1982) *Continental carbonate sedimentation and pedogenesis—Late Cretaceous and Early tertiary of Southern France*. Stuttgart: E. Schweizerbart'sche Verlagsbuchhandlung, p. 213.
- Freytet, P. & Verrecchia, E.P. (2002) Lacustrine and palustrine carbonate petrography: an overview. *Journal of Paleolimnology*, 27, 221–237.
- Fritz, M., Unkel, I., Lenz, J., Gajewski, K., Frenzel, P., Paquette, N., Lantuit, H., Körte, L. & Wetterich, S. (2018) Regional environmental change versus local signal preservation in Holocene thermokarst lake sediments: a case study from Herschel Island, Yukon (Canada). *Journal of Paleolimnology*, 60, 77–96. <https://doi.org/10.1007/s10933-018-0025-0>
- Fürsich, F.T. (1993) Palaeoecology and evolution of Mesozoic salinity-controlled benthic macroinvertebrate associations. *Lethaia*, 26, 327–346. <https://doi.org/10.1111/j.1502-3931.1993.tb01540.x>
- Gély, J.P. & Lorenz, C. (1991) Analyse séquentielle de l'Eocène et de l'Oligocène du bassin Parisien (France). *Revue de l'Institut Français du Pétrole*, 46, 713–747. (in French with English abstract). <https://doi.org/10.2516/ogst:1991034>
- Gély, J.P. (2016) The Paleogene of the Paris Basin: correlations and paleogeography. *Bulletin d'Information des Géologues du Bassin de Paris*, 53, 2–13 (in French with English abstract).
- Gierlowski-Kordesch, E.H. (2010) Chapter 1: lacustrine carbonates. In: Alonso-Zarza, A.M. & Tanner, L.H. (Eds.), *Developments in Sedimentology, Carbonates in continental settings: facies, environments, and processes*. Amsterdam: Elsevier, 61, pp. 1–101.
- Gigot, C. (1973) Carte géologique de la France à 1/50 000e (n°362), Patay, Notice explicative. BRGM, Orléans, 18 p.
- Gigot, C. (1980) Carte géologique de la France à 1/50 000e (n°292), Méréville, notice explicative. BRGM, Orléans, 26 p.
- Gigot, C. (1984) Carte géologique de la France à 1/50 000e (n°364), Bellegarde-du-Loiret, notice explicative. BRGM, Orléans, 32 p.
- Gitton, J.L., Lozouet, P. & Maestrati, P. (1986) Biostratigraphie et paléocologie des gisements types du Stampien de la région d'Etampes (Essonne). *Géologie de la France*, 1, 3–101 (in French with English abstract).
- Gradstein, F.M., Ogg, J.G., Schmitz, M.D. & Ogg, G.M. (Eds.). (2020) *Geologic time scale 2020*, 1st edition. Amsterdam: Elsevier, p. 584.
- Guan, X., Wu, C., Zhou, T., Tang, X., Ma, J. & Fang, Y. (2021) Jurassic–Lower Cretaceous sequence stratigraphy and allogenic controls in proximal terrestrial environments (Southern Junggar Basin, NW China). *Geological Journal*, 56, 4038–4062. <https://doi.org/10.1002/gj.4132>
- Guillemin, C. (1976) Les formations carbonatées dulçaquicoles tertiaires de la région centre (Briare, Chateau-Landon, Berry, Beauce). PhD thesis, Université d'Orléans, Orléans, 141 pp (in French).
- Guillocheau, F., Robin, C., Allemand, P., Bourquin, S., Brault, N., Dromart, G., Friedenber, R., Garcia, J.-P., Gaulier, J.-M., Gaumet, F., Grosdoy, B., Hanot, F., Le Strat, P., Mettraux, M., Nalpas, T., Prijac, C., Rigollet, C., Serrano, O. & Grandjean, G. (2000) Meso-Cenozoic geodynamic evolution of the Paris Basin: 3D stratigraphic constraints. *Geodinamica Acta*, 13, 189–245. <https://doi.org/10.1080/09853111.2000.11105372>
- Hamilton, D.S. & Tadros, N.Z. (1994) Utility of coal seams as genetic stratigraphic sequence boundaries in nonmarine basins: an example from the Gunnedah Basin, Australia. *AAPG Bulletin*, 78, 267–286. <https://doi.org/10.1306/BDF9082-1718-11D7-8645000102C1865D>
- Hanneman, D.L. & Wideman, C.J. (2010) Chapter 5: continental sequence stratigraphy and continental carbonates. In: Alonso-Zarza, A.M. & Tanner, L.H. (Eds.) *Developments in Sedimentology Carbonates in continental settings: geochemistry, diagenesis, and applications*, Vol. 62. Amsterdam: Elsevier, pp. 215–273. [https://doi.org/10.1016/S0070-4571\(09\)06205-0](https://doi.org/10.1016/S0070-4571(09)06205-0)
- Hardenbol, J., Thierry, J., Farley, M.B., Jacquin, T., de Graciansky, P.-C. & Vail, P.R. (1999) Mesozoic and cenozoic sequence chronostratigraphic framework of European Basins. Mesozoic and Cenozoic sequence stratigraphy of European Basins. *SEPM Special Publication*, 60, 3–15. <https://doi.org/10.2110/pec.98.02.0003>
- Huerta, P. & Armenteros, I. (2005) Calcrete and palustrine assemblages on a distal alluvial-floodplain: a response to local subsidence (Miocene of the Duero basin, Spain). *Sedimentary Geology*, 177, 253–270. <https://doi.org/10.1016/j.sedgeo.2005.03.007>
- Huyghe, D. (2010) Changements climatiques globaux et forçage tectonique au Paléogène: exemples du bassin de Paris et des Pyrénées au Paléogène. PhD thesis, Paris 6, Paris, 359 p (in French with English abstract).
- Huyghe, D., Lartaud, F., Emmanuel, L., Merle, D. & Renard, M. (2015) Palaeogene climate evolution in the Paris Basin from oxygen stable isotope ($\delta^{18}\text{O}$) compositions of marine molluscs. *Journal of the Geological Society*, 172, 576–587. <https://doi.org/10.1144/jgs2015-016>
- Kabanov, P., Anadón, P. & Krumbein, W.E. (2008) Microcodium: an extensive review and a proposed non-rhizogenic biologically induced origin for its formation. *Sedimentary Geology*, 205, 79–99. <https://doi.org/10.1016/j.sedgeo.2008.02.003>
- Keighley, D., Flint, S., Howell, J. & Moscariello, A. (2003) Sequence stratigraphy in lacustrine basins: a model for part of the Green River Formation (Eocene), Southwest Uinta Basin, Utah, U.S.A. *Journal of Sedimentary Research*, 73, 987–1006. <https://doi.org/10.1306/050103730987>
- Kendall, C.G.S.C. & Warren, J. (1987) A review of the origin and setting of tepees and their associated fabrics. *Sedimentology*, 34, 1007–1027. <https://doi.org/10.1111/j.1365-3091.1987.tb00590.x>
- Kosir, A. (2004) Microcodium revisited: Root calcification products of terrestrial plants on carbonate-rich substrates. *Journal of Sedimentary Research*, 74, 845–857. <https://doi.org/10.1306/040404740845>
- Labourguigne, J. (1971) Carte géologique de la France à 1/50 000e (n°153), Dammartin-en-Goële, Notice explicative. Orléans: BRGM, p. 26.

- Labourguigne, J. & Turland, M. (1974) Carte géologique de la France à 1/50 000e (n°258), Melun, Notice explicative. Orléans: BRGM, p. 29.
- Langer, M.R. & Lipps, J.H. (2003) Foraminiferal distribution and diversity, Madang Reef and Lagoon, Papua New Guinea. *Coral Reefs*, 22, 143–154. <https://doi.org/10.1007/s00338-003-0298-1>
- Leng, M.J. & Marshall, J.D. (2004) Palaeoclimate interpretation of stable isotope data from lake sediment archives. *Quaternary Science Reviews*, 23, 811–831. <https://doi.org/10.1016/j.quascirev.2003.06.012>
- Le Callonnec, L., Galbrun, B., Person, A., Harivel, C., Schnyder, J. & Baut, J.-P. (2018) Lagoon story at the Eocene–Oligocene boundary in the Paris Basin: Sedimentary series of the Cormeilles-en-Parisis quarry (France). *Bulletin d'Information des Géologues du Bassin de Paris*, 56, 3–21.
- Le Calvez, Y. (1970) Contribution à l'étude des foraminifères paléogènes du Bassin de Paris. In: *Cahiers de Paléontologie*. Paris: C.N.R.S., Éditions du Centre national de la recherche scientifique, pp. 1–326 (In French).
- Lettéron, A., Fournier, F., Hamon, Y., Villier, L., Margerel, J.-P., Bouche, A., Feist, M. & Joseph, P. (2017) Multi-proxy paleoenvironmental reconstruction of saline lake carbonates: Paleoclimatic and paleogeographic implications (Priabonian–Rupelian, Issirac Basin, SE France). *Sedimentary Geology*, 358, 97–120.
- Lettéron, A., Hamon, Y., Fournier, F., Séranne, M., Pellenard, P. & Joseph, P. (2018) Reconstruction of a saline, lacustrine carbonate system (Priabonian, St-Chaptes Basin, SE France): Depositional models, paleogeographic and paleoclimatic implications. *Sedimentary Geology*, 367, 20–47. <https://doi.org/10.1016/j.sedgeo.2017.12.023>
- Lettéron, A., Hamon, Y., Fournier, F., Demory, F., Séranne, M. & Joseph, P. (2022) Stratigraphic architecture of a saline lake system: From lake depocentre (Alès Basin) to margins (Saint-Chaptes and Issirac basins), Eocene–Oligocene transition, south-east France. *Sedimentology*, 69, 651–695. <https://doi.org/10.1111/sed.12920>
- Londeix, L., de Wever, P. & Cornée, A. (2014) *Stratotype aquitainien*. Paris: Museum national d'Histoire naturelle. pp. 416 (in French).
- Lozouet, P. (2012) *Stratotype Stampien*. Paris: Museum national d'Histoire naturelle. 461 p (in French).
- MacNeil, A.J. & Jones, B. (2006) Palustrine Deposits on a Late Devonian Coastal Plain—Sedimentary Attributes and Implications for Concepts of Carbonate Sequence Stratigraphy. *Journal of Sedimentary Research*, 76, 292–309. <https://doi.org/10.2110/jsr.2006.028>
- Marchand, J. (1968) Carte géologique de la France à 1/50 000e (n°221), Rozay-en-Brie, Notice explicative. BRGM, Orléans, 15 p.
- Marchegiano, M. & John, C.M. (2022) Disentangling the Impact of Global and Regional Climate Changes During the Middle Eocene in the Hampshire Basin: New Insights From Carbonate Clumped Isotopes and Ostracod Assemblages. *Paleoceanography and Paleoclimatology*, 37, 13. <https://doi.org/10.1029/2021PA004299>
- Mathelin, J.-C. & Bignot, G. (1989) Le falun de Foulangues et ses relations stratigraphique et paléogéographique avec le Biarritzien stratotypique. *Comptes rendus du Congrès National des Sociétés Savantes*, 114, 55–70. (in French).
- Mégnién, C. (1974) Le passage latéral du gypse au Calcaire de Champigny dans le nord de la Brie et son interprétation paléogéographique. *Bulletin d'Information des Géologues du Bassin de Paris*, 41, 47–65 (in French with English abstract).
- Mégnién, C. (1980) Synthèse géologique du bassin de Paris, Mémoires du Bureau de recherches géologiques et minières. No. 101–103, Editions du BRGM (in French).
- Melo, A.H., Magalhães, A.J.C., Menegazzo, M.C., Fragoso, D.G.C., Florencio, C.P. & Lima-Filho, F.P. (2021) High-resolution sequence stratigraphy applied for the improvement of hydrocarbon production and reserves: A case study in Cretaceous fluvial deposits of the Potiguar basin, northeast Brazil. *Marine and Petroleum Geology*, 130, 105124. <https://doi.org/10.1016/j.marpetgeo.2021.105124>
- Ménillet, F. (1974) Etude pétrographique et sédimentologique des calcaires d'Etampes et de Beauce, formations dulçaquicoles du Stampien supérieur à l'Aquitainien dans le Bassin de Paris. PhD thesis, Paris Sud, Paris, 138 pp (in French).
- Mercedes-Martín, R., Arenas, C. & Salas, R. (2014) Diversity and factors controlling widespread occurrence of syn-rift Ladinian microbialites in the western Tethys (Triassic Catalan Basin, NE Spain). *Sedimentary Geology*, 313, 68–90. <https://doi.org/10.1016/j.sedgeo.2014.08.006>
- Merle, D. (2008) Stratotype Lutétien. Paris: Museum national d'Histoire naturelle, pp. 288 (in French).
- Meulenkamp, J.E., Sissingh, W., Londeix, L., Cahuzac, B. & Calvo, J.P. (2000) Late Lutetian, Late Rupelian. In: Dercourt, J., Gaetani, M., Vrielynck, B., Barrier, E., Biju-Duval, B., Brunet, M.F., Cadet, J.P., Crasquin, S. & Sandulescu, M. (Eds.) *Atlas peri-tethys. Palaeogeographical maps*, Explanatory notes. Paris: CCGM/CGMW, pp. 163–178.
- Miller, C.R., James, N.P. & Kyser, T.K. (2013) Genesis of blackened limestone clasts at Late Cenozoic subaerial exposure surfaces, Southern Australia. *Journal of Sedimentary Research*, 83, 339–353. <https://doi.org/10.2110/jsr.2013.32>
- Miller, K., Schmelz, J., Browning, J., Kopp, R., Mountain, G. & Wright, J. (2020) Ancient sea level as key to the future. *Oceanography*, 33, 32–41. <https://doi.org/10.5670/oceanog.2020.224>
- Morellet, L. & Morellet, J. (1948) Le Bartonien du bassin de Paris. *Mémoires pour servir à l'explication de la Carte Géologique de la France*, 39, pp. 437 (in French).
- Pemberton, S.G., MacEachern, J.A. & Frey, R.W. (1992) Trace fossil facies models; environmental and allostratigraphic significance. In: Walker, R.G. & James, N.P. (Eds.) *Facies model*. Toronto: Geological Association of Canada, pp. 47–72.
- Pérez-Rivarés, F.J., Arenas, C., Pardo, G. & Garcés, M. (2018) Temporal aspects of genetic stratigraphic units in continental sedimentary basins: examples from the Ebro basin, Spain. *Earth Science Reviews*, 178, 136–153. <https://doi.org/10.1016/j.earscirev.2018.01.019>
- Pint, A., Engel, M., Melzer, S., Frenzel, P., Plessen, B. & Brückner, H. (2017) How to discriminate athalassic and marginal marine microfaunas: Foraminifera and other fossils from an Early Holocene continental lake in Northern Saudi Arabia. *Journal of Foraminiferal Research*, 47, 175–187. <https://doi.org/10.2113/gsjfr.47.2.175>
- Platt, N.H. (1989) Lacustrine carbonates and pedogenesis: Sedimentology and origin of palustrine deposits from the Early Cretaceous Rupelo Formation, W Cameros Basin, N Spain.

- Sedimentology*, 36, 665–684. <https://doi.org/10.1111/j.1365-3091.1989.tb02092.x>
- Platt, N.H. & Wright, V.P. (1991) Lacustrine carbonates: facies models, facies distributions and hydrocarbon aspects. *Special Publications of the International Association*, 13, 57–74. <https://doi.org/10.1002/9781444303919.ch3>
- Platt, N.H. & Wright, V.P. (1992) Palustrine carbonates and the Florida Everglades: towards an exposure index for the fresh-water environment? *Journal of Sedimentary Research*, 62, 1058–1071. <https://doi.org/10.1306/D4267A4B-2B26-11D7-8648000102C1865D>
- Platt, N.H. & Wright, V.P. (2023) Flooding of a carbonate platform: The Sian Ka'an Wetlands, Yucatán, Mexico—a model for the formation and evolution of palustrine carbonate factories around the modern Caribbean Sea and in the depositional record. *Depositional Record*, 9, 99–151. <https://doi.org/10.1002/dep2.217>
- Plaziat, J.-C. (1993) Modern and fossil Potamids (Gastropoda) in saline lakes. *Journal of Paleolimnology*, 8, 163–169. <https://doi.org/10.1007/BF00119788>
- Pomerol, C., Damotte, R., Ginsburg, L., Montenat, C., Lorenz, J. & Toutin, N. (1965) Etude paléontologique et sédimentologique du Bartonien inférieur (Auversien) dans la localité-type du Guepelle (Seine-et-Oise). *Bulletin de la Société Géologique de France*, 7, 257–267 (in French).
- Pomerol, C. & Riveline, J. (1975) Etude floristique (Characée) des calcaires de Mortemer et de Cuvilly dans leurs localités-types. *Comptes Rendus Hebdomadaires des Séances de l'Académie des Sciences, Série D: Sciences Naturelles*, 280, 2725–2728 (in French).
- Pomerol, C. (1989) Stratigraphy of the Palaeogene; Hiatuses and transitions. *Proceedings of the Geologists' Association*, 100, 313–324. [https://doi.org/10.1016/S0016-7878\(89\)80051-3](https://doi.org/10.1016/S0016-7878(89)80051-3)
- Riveline, J. (1983) Proposition d'une échelle zonale de Charophytes pour le Tertiaire (Danien à Burdigalien) d'Europe occidentale. *Comptes Rendus. Académie des Sciences*, 296, 1077–1080.
- Riveline, J., Berger, J.-P., Feist, M., Martin-Closas, C., Schudack, M. & Soulié-Marsche, I. (1996) European Mesozoic-Cenozoic charophyte biozonation. *Bulletin de la Société Géologique de France*, 167, 453–468.
- Robin, C., Guillocheau, F. & Gaulier, J.M. (1998) Discriminating between tectonic and eustatic controls on the stratigraphic record in the Paris basin. *Terra Nova*, 10, 323–329. <https://doi.org/10.1046/j.1365-3121.1998.00210.x>
- Roche, A., Vennin, E., Bouton, A., Olivier, N., Wattinne, A., Bundeleva, I., Deconinck, J.-F., Virgone, A., Gaucher, E.C. & Visscher, P.T. (2018) Oligo-Miocene lacustrine microbial and metazoan buildups from the Limagne Basin (French Massif Central). *Palaeogeography Palaeoclimatology Palaeoecology*, 504, 34–59. <https://doi.org/10.1016/j.palaeo.2018.05.001>
- Roche, A. (2020) Dépôts carbonatés microbiens en domaine lacustre et fluvial: fabriques et facteurs de contrôle, PhD thesis. Bourgogne Franche-Comté, Dijon, 360 pp. (in French).
- Rouchy, J.M., Camoin, G., Casanova, J. & Deconinck, J.F. (1993) The central palaeo-Andean basin of Bolivia (Potosi area) during the Late Cretaceous and Early Tertiary: Reconstruction of ancient saline lakes using sedimentological, paleoecological and stable isotope records. *Palaeogeography Palaeoclimatology Palaeoecology*, 105, 179–198. [https://doi.org/10.1016/0031-0182\(93\)90083-U](https://doi.org/10.1016/0031-0182(93)90083-U)
- Rouchy, J.M., Taberner, C. & Peryt, T.M. (2001) Sedimentary and diagenetic transitions between carbonates and evaporites. *Sedimentary Geology*, 140, 1–8. [https://doi.org/10.1016/S0037-0738\(00\)00169-X](https://doi.org/10.1016/S0037-0738(00)00169-X)
- Scherler, L., Mennecart, B., Hiard, F. & Becker, D. (2013) Evolutionary history of hoofed mammals during the Oligocene–Miocene transition in Western Europe. *Swiss Journal of Geosciences*, 106, 349–369.
- Schreiber, B.C. (1988) Chapter 4: subaqueous evaporite deposition. In: *Evaporites and hydrocarbons*. New York: Columbia University Press, pp. 182–255.
- Shaw, P.A., Cooke, H.J. & Perry, C.C. (1990) Microbialitic silcretes in highly alkaline environments: Some observations from Sua Pan, Botswana. *South African Journal of Geology*, 93, 803–808.
- Speijer, R.P., Pälike, H., Hollis, C.J., Hooker, J.J. & Ogg, J.G. (2020) Chapter 28: the paleogene period. In: Gradstein, F.M., Ogg, J.G., Schmitz, M.D. & Ogg, G.M. (Eds.) *Geologic time scale 2020*. Amsterdam: Elsevier, pp. 1087–1140. <https://doi.org/10.1016/B978-0-12-824360-2.00028-0>
- Strasser, A. (1984) Black-pebble occurrence and genesis in Holocene carbonate sediments (Florida Keys, Bahamas, and Tunisia). *Journal of Sedimentary Research*, 54, 1097–1109. <https://doi.org/10.1306/212F856C-2B24-11D7-8648000102C1865D>
- Strecker, U., Steidtmann, J.R. & Smithson, S.B. (1999) A conceptual tectonostratigraphic model for seismic facies migrations in a fluvio-lacustrine extensional basin. *AAPG Bulletin*, 83, 43–61. <https://doi.org/10.1306/00AA99F8-1730-11D7-8645000102C1865D>
- Strotz, L.C. (2015) Spatial patterns and diversity of foraminifera from an intermittently closed and open lagoon, Smiths Lake, Australia. *Estuarine, Coastal and Shelf Science*, 164, 340–352.
- Talbot, M.R. (1990) A review of the palaeohydrological interpretation of carbon and oxygen isotopic ratios in primary lacustrine carbonates. *Chemical Geology: Isotope Geoscience Section*, 80, 261–279. [https://doi.org/10.1016/0168-9622\(90\)90009-2](https://doi.org/10.1016/0168-9622(90)90009-2)
- Tandon, S.K. & Andrews, J.E. (2001) Lithofacies associations and stable isotopes of palustrine and calcrete carbonates: examples from an Indian Maastrichtian regolith. *Sedimentology*, 48, 339–355. <https://doi.org/10.1046/j.1365-3091.2001.00367.x>
- Thompson, D.L., Stilwell, J.D. & Hall, M. (2015) Lacustrine carbonate reservoirs from Early Cretaceous rift lakes of Western Gondwana: Pre-Salt coquinas of Brazil and West Africa. *Gondwana Research*, 28, 26–51. <https://doi.org/10.1016/j.jgr.2014.12.005>
- Toulemont, M. (1982) Les épigénies siliceuses du gypse lutétien du Bassin de Paris. *Sciences Géologiques Bulletin (Strasbourg)*, 35, 3–16 (in French). <https://doi.org/10.3406/sgeol.1982.1606>
- Turland, M. (1974) Etude géologique des terrains tertiaires de la région de Montereau (Seine-et-Marne). PhD thesis, Paris, 135 pp. (in French).
- Utescher, T., Mosbrugger, V. & Ashraf, A.R. (2000) Terrestrial climate evolution in northwest Germany over the last 25 million years. *Palaios*, 15, 430–449.
- Vail, P.R., Audemard, F., Bowman, S.A., Eisner, P.N. & Perez-Cruz, C. (1991) The stratigraphic signatures of tectonics, eustasy and sedimentology—an overview. In: Einsele, G., Ricken, W. & Seilacher, A. (Eds.) *Cycles and events in stratigraphy*, Berlin: Springer, pp. 617–659.
- Vennin, E., Bouton, A., Roche, A., Gérard, E., Bundeleva, I., Boussagol, P., Wattinne, A., Kolodka, C., Gaucher, E., Virgone, A. & Visscher, P.T. (2021) The Limagne Basin: a journey through modern and

- fossil microbial deposits. *Bulletin de la Société géologique de France*, 192, 41. <https://doi.org/10.1051/bsgf/2021030>
- Vera, J.A. & Jiménez de Cisneros, C. (1993) Palaeogeographic significance of black pebbles (Lower Cretaceous, Prebetic, southern Spain). *Palaeogeography Palaeoclimatology Palaeoecology*, 102, 89–102. [https://doi.org/10.1016/0031-0182\(93\)90007-6](https://doi.org/10.1016/0031-0182(93)90007-6)
- Warren, J.K. & Kendall, C.G.S.C. (1985) Comparison of sequences formed in marine Sabkha (Subaerial) and salina (subaqueous) settings—modern and ancient. *AAPG Bulletin*, 69, 1013–1023. <https://doi.org/10.1306/AD462B46-16F7-11D7-8645000102C1865D>
- Wilson, J.L. (1974) Characteristics of carbonate-platform margins. *AAPG Bulletin*, 58, 810–824. <https://doi.org/10.1306/83D9149D-16C7-11D7-8645000102C1865D>
- Wright, V.P., Platt, N.H. & Wimbledon, W.A. (1988) Biogenic laminar calcretes: evidence of calcified root-mat horizons in paleosols. *Sedimentology*, 35, 603–620.
- Wright, V.P. (1989) Terrestrial stromatolites and laminar calcretes: a review. *Sedimentary Geology*, 65, 1–13.
- Wright, V.P. & Tucker, M.E. (1991) Calcretes: an Introduction. In: Wright, V.P. & Tucker, M.E. (Eds.) *Calcretes*. Oxford: Blackwell Publishing Ltd, pp. 1–22. <https://doi.org/10.1002/9781444304497.ch>
- Wright, V.P. (1994) Paleosols in shallow marine carbonate sequences. *Earth Science Reviews*, 35, 367–395. [https://doi.org/10.1016/0012-8252\(94\)90002-7](https://doi.org/10.1016/0012-8252(94)90002-7)
- Ziegler, P.A. (1990) *Geological atlas of Western and Central Europe*. London: Shell International Petroleum Mij. B.V. and Geological Society, Bath, p. 239.

SUPPORTING INFORMATION

Additional supporting information can be found online in the Supporting Information section at the end of this article.

How to cite this article: Moreau, K., Andrieu, S., Briaux, J., Brigaud, B. & Ader, M. (2023) Facies distribution and depositional cycles in lacustrine and palustrine carbonates: The Lutetian–Aquitainian record in the Paris Basin. *The Depositional Record*, 00, 1–35. Available from: <https://doi.org/10.1002/dep2.264>